Science of the Total Environment 613–614 (2018) 271–286

Contents lists available at ScienceDirect

Science of the Total Environment

journal homepage: www.elsevier.com/locate/scitotenv

Freshwater vulnerability under high end climate change. A pan-European assessment

A.G. Koutroulis [a,*], L.V. Papadimitriou [a], M.G. Grillakis [a], I.K. Tsanis [a], K. Wyser [b], R.A. Betts [c]

[a] Technical University of Crete, School of Environmental Engineering, Chania, Greece
[b] Rossby Centre, Swedish Meteorological and Hydrological Institute, Norrköping, Sweden
[c] College of Life and Environmental Sciences, University of Exeter, Exeter EX4 4QE, United Kingdom

HIGHLIGHTS

- A Pan-EU conceptual framework for freshwater vulnerability is proposed.
- The approach can support regional level policy making and implementation.
- Most vulnerable countries should invest in human capital.

GRAPHICAL ABSTRACT

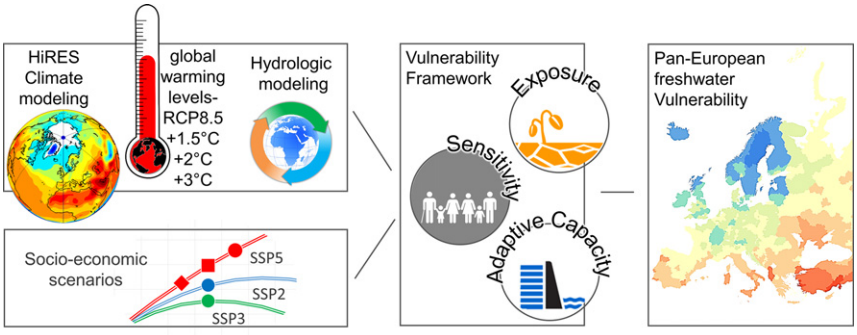

ARTICLE INFO

Article history:
Received 21 July 2017
Received in revised form 8 September 2017
Accepted 8 September 2017
Available online 14 September 2017

Editor: D. Barcelo

Keywords:
Water availability
Droughts
Adaptation
Vulnerability
Europe

ABSTRACT

As freshwater availability is crucial for securing a sustainable, lower carbon future, there is a critical connection between water management and climate policies. Under a rapidly changing climate, it is more important than ever to estimate the degree of future water security. This is a challenging task as it depends on many different variables: the degree of warming and its consequent effects on hydrological resources, the water demand by different sectors, and the possible ameliorations or deteriorations of the effects due to climate change adaptation and mitigation strategies. A simple and transparent conceptual framework has been developed to assess the European vulnerability to freshwater stress under the present hydro-climatic and socioeconomic conditions, in comparison to projections of future vulnerability for different degrees of global warming (1.5 °C, 2 °C and 4 °C), under the high-rate warming scenario (RCP8.5). Different levels of adaptation to climate change are considered in the framework, by employing various relevant pathways of socioeconomic development. A spatially detailed pan-European map of vulnerability to freshwater shortage has been developed at the local administrative level, making this approach extremely useful for supporting regional level policymaking and implementation and strategic planning against future freshwater stress.

1. Introduction

Recent climate policies might need to be revised to reach the goals established with the Paris Agreement. State of the art climate projections show that the higher-end climate change scenarios progressively become more probable as the projected warming considerably surpasses

* Corresponding author.
E-mail address: aris@hydromech.gr (A.G. Koutroulis).

http://dx.doi.org/10.1016/j.scitotenv.2017.09.074
0048-9697/

the 2 °C target. Under such circumstances, the availability of hydrological resources emanates as a vital subject that policy makers will have to manage (Papadimitriou et al., 2016). Future water security is challenging to estimate as it depends on many different variables, such as the degree of global warming and its consequent effects on hydrological resources, the water demand by different sectors, and the possible ameliorations or deteriorations of the effects due to climate change adaptation and mitigation strategies. Climate affects freshwater availability and simultaneously changes the social stress on it, which in turn affects socioeconomic variables that also affect climate. To cope with these complex interactions, socio-economic scenarios are used to derive emissions pathways without (reference) and with climate policies (mitigation scenarios). The derived emissions are then used as input to climate models, to obtain climate change projections. Finally, the climate change projections and socio-economic scenarios are used to evaluate the impact of climate change in combination with adaptation measures. A concept for the assessment of climate change impacts under adaptation strategies is the estimation of vulnerability.

According to the fourth IPCC assessment report (Parry, 2007) vulnerability is a measure of a system's susceptibility to, and inability to cope with, unfavourable climate change impacts, such as climate variability and extremes. Vulnerability is often decomposed into the three major components of exposure, sensitivity and adaptive capacity (Preston and Scientific, 2008) and in the context of climate change depends on the type, magnitude, and rate of change. These constituents of vulnerability -sensitivity, exposure and adaptive capacity- are interrelated and have wide applications in studying environmental changes providing many insights at global, regional or local scale (Smit and Wandel, 2006). The adoption of this concept by the IPCC leads to the "mainstreaming" of adaptation to the concept of many studies dealing with climate change. Although the concept of vulnerability assessment is a widespread methodology of examining the degree of exposure for many environmental systems under change (Turner et al., 2003), the application to drought is not a widespread practice, suggesting the need of increased effort (González Tánago et al., 2016). One of the main reasons is the difficulty in retrieving quantitative information on drought damages and vulnerability (Blauhut et al., 2015). González Tánago et al. (2016) conducted a systematic review of the drought vulnerability assessments in the scientific literature until mid-2015 revealing the broad diversity of the underlying conceptual frameworks and the lack of accordance on the kind and the amount of factors and dimensions that need to be analyzed.

Indicative recent studies on drought vulnerability at the global scale are presented below. Carrão et al. (2016) elaborated on a drought risk map, by combining independent indicators of historical droughts and estimates of drought exposure and vulnerability, finding that potential drought risk is mostly driven by the growth of regional exposure. A more focused approach on world's cereal producing regions was applied to identify vulnerability hotspots following a systematic drought vulnerability assessment framework (Fraser et al., 2013). Naumann et al. (2014) explored different aspects of drought vulnerability using a composite indicator for the identification of drought hotspots over Africa. A good agreement of mapped drought vulnerability and disaster information from the EM-DAT database was established.

Several systematic vulnerability assessment studies have been developed and applied at a continental, regional or national scale over Europe. Alcamo et al. (2008) used inference modeling to capture the susceptibility to drought by quantifying crucial vulnerability indicators. Iglesias et al. (2009) presented components-indices for evaluating social vulnerability to drought and the effect of index weighting through an application to six Mediterranean countries. Salvati et al. (2009) applied a comprehensive framework of mapping vulnerability of land to drought and desertification by combining biophysical and socioeconomic indicators over Italy. Flörke et al. (2011) used a similar to the present study approach to describe the change in European drought vulnerability by the 2050s under the A1B scenario. Perčec Tadić et al. (2014) developed a drought vulnerability map for Croatia based on climatic and geophysical indicators giving a first insight of the drought sensitive areas. The extensive work of the DROUGHT R&SPI FP7 project (Stagge, 2015) provided a systematic categorization of environmental and socioeconomic factors affecting vulnerability and can be used for developing an assessment framework. Blauhut et al. (2016) used several indicators of the previous study for the development of a hybrid framework of probabilistic impact prediction combined with vulnerability assessment for monitoring drought risk at a pan-European level.

Here, a simple and transparent conceptual framework for the assessment of European freshwater vulnerability is developed and applied. Vulnerability to freshwater stress is firstly assessed with respect to current hydro-climatic and socioeconomic conditions and is then compared to future vulnerability, projected for different degrees of global warming (1.5 °C, 2 °C and 4 °C), under the high-rate warming scenario (RCP8.5). Projected vulnerability is estimated for different level of adaptation to climate change, by employing various relevant socioeconomic pathways (SSP2, SSP3 and SSP5).

2. Data and methods

2.1. Forcing datasets

The forcing datasets used for this study are an ensemble of global high resolution climate model simulations, generated with the use of the EC-Earth3-HR model (Alfieri et al., 2017) in Atmospheric General Circulation Model (AGCM) mode. EC-Earth3-HR was run with prescribed sea surface temperature (SST) and sea–ice concentration, provided by six CMIP5 models. The criterion for model selection was to cover a wide range of uncertainty in the future climate projections. The ensemble includes two models of respectively high and low climate sensitivity (IPSL-CM5A-LR and GFDL-ESM2M), a dry (IPSL-CM5A-MR) and a wet (GISS-E2-H) model and finally two additional global climate models (HadGEM2-ES and EC-EARTH). The selection of the forcing models is based on an analysis of the historical and RCP8.5 results of all CMIP5 models that was done in the HELIX project (www.helixclimate.eu). The climate model output starts from the reference period and spans up to 2100 or 2120 for some models, in order to cover the time-periods that correspond to the examined warming levels (up to +4 °C). One model realization (r2, GFDL-ESM2M) is omitted from the SWL4 impacts' analysis as there were not data available for the SWL4 time-slice. The list of the CMIP5 models used to force the high–resolution climate simulations along with the time of exceedance of three examined Specific Warming Levels (SWLs) for each model are reported in Table 1. The native resolution of the simulation was 0.4°, regridded to 0.5° to fit the PGFv2 (Sheffield et al., 2006) observational dataset that was used as reference for the bias adjustment. The dataset assimilates a range of data sources. These are NCEP–NCAR reanalysis (Kalnay et al., 1996), CRU TS2.0 (Mitchell et al., 2004), GPCP (Huffman et al., 2001), TRMM (Huffman et al., 2007; Huffman and Bolvin, 2013) and NASA Langley SRB (Stackhouse et al., 2000). At a first stage, the reanalysis data variables were bilinearly interpolated to a 2.0° regular grid and the produced gridded dataset was commensurate with the other observation-based datasets. The daily timestep statistics are then adjusted by a series of

Table 1
CMIP5 forcing models used to force global high resolution atmosphere only simulations and year when each model exceeds the examined SWLs according to the RCP8.5 scenario.

Member	Forcing model	Ensemble member	SWL1.5	SWL2	SWL4
r1	IPSL-CM5A-LR	r1i1p1	2015	2030	2068
r2	GFDL-ESM2M	r1i1p1	2040	2055	2113
r3	HadGEM2-ES	r1i1p1	2027	2039	2074
r4	EC-EARTH	r12i1p1	2019	2035	2083
r5	GISS-E2-H	r1i1p1	2022	2038	2102
r6	IPSL-CM5A-MR	r1i1p1	2020	2034	2069

bias correction steps. The data are finally downscaled to a finer resolution with simultaneous temporal disaggregation.

The bias correction of the high resolution GCM data was performed using the ISI-MIP approach of trend-preserving bias correction (Hempel et al., 2013). The absolute changes of monthly temperature are preserved, as well as relative changes in monthly precipitation with the application of this methodology. The preservation in the long term trends is a desired feature of the bias adjustment methodology as the scenarios employed here are based on specific warming levels (Grillakis et al., 2017). Thus in the case of temperature, the bias adjusted data should preserve the warming levels of the raw climate model data and hence the climate sensitivity of the climate model. The same methodology was also used to correct a range of variables such as downward radiation, pressure and wind. In the case of positively constrained data such as precipitation, the method considers the preservation of the relative trend. The distribution of the estimated factors across all GCM realizations, that were used for the correction are presented in the Figure ESM25 included in the supplementary information document.

2.2. Time-slices

Climate change impacts are examined as differences between the temporal mean states of a future time-slice, corresponding to a SWL, and the reference period. It is important to mention that the SWLs are defined with respect to the pre-industrial period while the reference period corresponds to the recent past. All the examined time periods include 30 years. The reference (or baseline) period spans from 1981 to 2010. The future time-slices are 30-year periods, centering on the year that each SWL is exceeded.

2.3. Plausible combinations of RCP8.5 to SSP scenarios

In the present work, the RCP8.5 scenario was only considered, as the only one that can provide results of higher end global warming. However, the RCP8.5 is plausible under only specific socioeconomic assumptions, or Shared Socioeconomic Pathways (SSPs) (Arnell et al., 2011a, 2011b; Koutroulis et al., 2016; Moss et al., 2010). The scenario was assessed along with the SSP2, SSP3 and SSP5 scenarios.

2.4. Hydrological model

JULES (Joint UK Land Environment Simulator) is a fully distributed, physically based land-surface model that calculates the water, energy and carbon budget for each grid box included in the modeling domain. A detailed description of the model can be found in (Best et al., 2011) and (Clark et al., 2011), while a brief description of the main features of the model is given here.

JULES requires a number of meteorological forcing variables as input, namely: downward shortwave and longwave radiation components, precipitation rate, air temperature, wind-speed, air pressure and specific humidity (Best et al., 2011). The model consists of a number of modules that describe various physical processes (such as surface exchange of energy fluxes, snow cover, surface hydrology, soil moisture and temperature, plant physiology and soil carbon) (Best et al., 2011). Plant physiology is included in the model, meaning that transpiration will respond to rising CO_2 concentrations as well as the changing climate. This is an important feature of JULES that distinguishes it from pure hydrological models, as it has the ability to simulate both ecosystems and hydrology.

In JULES, land surface heterogeneity is introduced by using nine surface types (Best et al., 2011), five of which represent vegetation (broadleaf trees, needle leaf trees, C3 (temperate) grasses, C4 (tropical) grasses and shrubs) and the remaining four are non-vegetated surface types (urban, inland water, bare soil and ice). In JULES the default soil configuration (used in the present study) consists of four soil layers. The fluxes of soil moisture between each soil layer are calculated as Darcian fluxes and soil hydrology calculations are based on Richards' equation (Richards, 1931). Runoff production has two components: surface runoff, which is estimated with the infiltration excess mechanism, and sub-surface runoff, which is the drainage through the bottom of the soil column (Best et al., 2011). Potential evaporation is calculated according to the Penman-Monteith approach (Penman, 1948). The plant canopy water evaporates freely while evaporation from soil and plant transpiration is subject to restrictions of canopy resistance and soil moisture.

The processes within JULES model have been calibrated and validated in a number of previous studies against different observational and proxy datasets (e.g. Slevin et al., 2014; Pacifico et al., 2011; Garcia Gonzalez et al., 2012; Chadburn et al., 2015). Specifically for hydrological applications, various studies have tested its ability to simulate runoff generation (Gudmundsson et al., 2012; MacKellar et al., 2013; Papadimitriou et al., 2015). Moreover, the JULES model has been used in a number of climate change impacts studies that deal with the climate change response in hydrological regime (Le Vine et al., 2016; Papadimitriou et al., 2016; Zulkafli et al., 2013), the change in the soil temperature regime in global scale (Grillakis et al., 2016). The model setup used in the present study is described in the supplementary information.

2.5. Characterization of short and long term droughts

The standardized precipitation index (SPI, Mckee et al., 1993) is a widely used index for the identification of drought events' onset, intensity and duration. The calculation of the SPI is based on time series of precipitation. First the time series are fitted to a Gamma distribution and then the cumulative probability of precipitation values is estimated. Finally, the cumulative probability is transformed to a standard normal deviate with zero mean and unit standard deviation (Mckee et al., 1993). Negative values of SPI indicate the existence of drought conditions. According to the SPI value, drought is grouped into one of four arbitrarily defined intensity tiers, ranging from “mild” to “extreme” (Mckee et al., 1993). Following the SPI concept, Shukla and Wood (2008) developed the standardized runoff index, which characterizes droughts by assessing modeled runoff time series. SRI integrates hydrological mechanisms that can diminish and/or delay the effect of climate on discharge and can serve as an indicator of hydrological drought providing additional information especially in the case of short time scales. This work was focused on intense drought conditions, thus only the “severe drought” ($-2 < \mathrm{SPI} \leq -1.5$) and “extreme drought” ($\mathrm{SPI} \leq -2$) categories were considered. For the assessment of climate change impact on droughts we used the relative versions of SPI and SRI (Dubrovsky et al., 2009). Relative indices use input data of two time periods. The first period serves as the reference period and is used for model calibration. The calibrated model is then applied to data of the second time period. This allows us to assess the drought conditions of the future compared to the benchmark drought conditions of the baseline period. The relative drought indices were calculated using two periods of temporal aggregation (6 and 48 months), in order to capture droughts of different duration.

2.6. Development of a conceptual framework for assessing vulnerability

Most of the approaches of the current studies on drought vulnerability originate by two different schools (González Tánago et al., 2016). The first is the climate change adaptation school (CCA) that focuses on the level of a system's susceptibility to negative drought impacts. The second is the disaster reduction risk (DRR) school that examines the capacity of a person or group to prepare for, resist and cope with a hazardous event, and also restore its balance after the event has been terminated.

As a basis for the present study we adopted the approach of the CCA school and we followed the corresponding conceptualization similar to the one provided by the IPCC Fourth Assessment Report (Parry, 2007), which defines vulnerability as a function of three major components: the exposure to climate change, the sensitivity, and the adaptive capacity. The drought vulnerability from different levels of global warming

(+1.5 °C, +2 °C, +4 °C) is assessed with the use of an index approach accounting for the exposure, the sensitivity and the adaptive capacity at a pan-European NUTS2 level (Geographical nomenclature of territorial units subdividing the economic territory of the European Union, based on existing national administrative subdivisions). The assessment of vulnerability provides a qualitative view of climate risk rather than explicit predictions of climate change outcomes or impacts. Since the various climate, demographic and socioeconomic indicators are measured in different units, they are all brought to a common scale using an appropriate normalization method. Several normalization methods can be found in literature, each with specific advantages and disadvantages (Fekete, 2009). The decile normalization was selected for its robustness and simplicity. The method categorizes the data of each indicator into deciles and assigns score from 1 to 10. Table 2 includes the indicators and corresponding expressions of exposure, sensitivity and adaptive capacity of European vulnerability to drought used in the scoring framework. We adopted a non-stationary scoring approach to account for changes in indicators beyond the baseline period that was applied prior the decile normalization.

The resulting indicators for the dimensions of exposure, sensitivity and adaptive capacity were equally weighted by 1/3. Equal weighting was also applied for all sub-indices of each dimension. This standard equal weighting procedure was chosen for the sake of subjectivity. The weights assigned to the model dimensions and indices are included in Table 2.

2.6.1. Exposure indicators

Exposure, in the context of climate change, describes the type and the level of a system's exposure to substantial climate variability (Füssel and Klein, 2006). Different elements in which hazardous events may occur comprise the elements inventory of exposure (Birkmann et al., 2014). In practice, the exposure is conceived as the changes in the climate variability and/or the climate system (Brooks et al., 2005).

2.6.1.1. Water availability on average. A first indicator of exposure to water stress is freshwater availability. In this study, freshwater availability is described by runoff production (Papadimitriou et al., 2016). Runoff production is derived from the hydrological simulations forced by the EC-EARTH-HR climate model runs.

2.6.1.2. Low flows. A second indicator that is capable to describe the exposure to water stress is the information on low flow regimes (Prudhomme et al., 2011). While the change in the low flows is also part of the change in the mean runoff production, it serves for the indication of trends of more intense or/and often extreme lows in the projected water budget (Papadimitriou et al., 2016).

2.6.1.3. Short and long term droughts. Additionally to the abovementioned indicators, drought indices like the standardized precipitation index (SPI) can effectively map the duration and severity of the extreme meteorological droughts (Stagge et al., 2015) relevant to water availability and can also facilitate the concept of exposure indicator in the vulnerability assessment framework. The 6-months temporal scale was selected for the examination of short term meteorological drought associated to agricultural drought and changes to the seasonal variations. The 48-months temporal scale was employed for the description of long term droughts and effects on high capacity reservoirs related to drought indices at long time scales (Lorenzo-Lacruz et al., 2010). Exposure to short term and long term hydrological drought was examined with the use of 6-months and 48-months SRI temporal scales, respectively. SRI was employed in order to provide additional information on exposure by capturing hydrological processes and associated droughts which cannot be described by SPI (meteorological drought).

2.6.2. Sensitivity indicators

The sensitivity of water availability and stress in climate change refers to the responsiveness of the socioeconomic system to the related climate induced hazards. Their responsiveness on climate induced changes can be estimated by a series of indicators that represent the degree that they are exposed to climate change.

2.6.2.1. Population density. Population density has been found to serve as an appropriate indicator of pressure on the environment in terms of water resources related hazards (Kossida et al., 2012), serving as a two-fold indicator. A densely populated region is more susceptible to water related natural disasters such as droughts, as more people will be affected by it per unit area (Cutter and Finch, 2008; Yohe and Tol, 2002). At the same time the infrastructure capacity is a function of population density, with the former to be increasingly sensitive by its size on water related hazards. Furthermore, potential changes in population density can lead to changes in water demand (Kossida et al., 2012; Leary and Kulkarni, 2007).

2.6.2.2. Irrigated agriculture. Approximately 70% of the global freshwater withdrawals are currently used in agriculture. The respective usage in Europe is 21% while it varies significantly along the European region, from the northern countries where precipitation is relatively equally distributed through the year and irrigation withdrawals may even be negligible, to the southern countries where the precipitation presents a highly seasonal pattern and the irrigation water reaches to as high as 70% of the available water. Hence irrigation is a major consumer of freshwater in parts of Europe, especially in the southern regions. The sensitivity of agricultural areas was expressed as the fraction of the cultivated area that is irrigated, at NUTS2 level. Irrigated area fractions (as a percentage) were obtained from FAO's AQUASTAT website.

2.6.2.3. Water demand sectorial. Additionally, past and future sectorial water demand was included in the vulnerability analysis. This indicator

Table 2
Indicators and expressions of exposure, sensitivity and adaptive capacity of vulnerability to freshwater scarcity.

	Indicator	Expressed by	Weight
Exposure	Water availability on average	Relative changes in mean annual runoff production	1/4
	Low flows	Relative changes in 10th percentile runoff production	1/4
	Duration and severity of extreme events relevant to water availability (short and long term droughts)	Change in duration of short and long term *meteorological* droughts – index based on standardized precipitation index (SPI) of 6 and 48 months temporal scale	1/4
		Change in duration of short and long term *hydrological* droughts – index based on standardized runoff index (SRI) of 6 and 48 months temporal scale	1/4
Sensitivity	Population density	Number of people totally affected by freshwater stress	1/3
	Irrigated agriculture	Extend of irrigated area - FAO	1/3
	Water Demand sectorial	Gridded dataset of water demand per sector	1/3
Adaptive capacity	Economic resources available to adapt	GDP per capita (PPP)	1/5
	Law enforcement	World Governance Indicators (WGI) - World Bank	1/5
	Human Capital	Percent of highly educated working population	1/5
	Level of natural freshwater storage capacity	Extend of highly productive aquifers and inland water bodies for freshwater storage	1/5
	Level of artificial freshwater storage capacity	Storage capacity of dams. Geo-referenced dataset for Europe - FAO	1/5

can express the human stress posed on the available freshwater. Hanasaki et al. (2013), used the statistics-based national water withdrawal data for domestic, industrial, and agricultural sectors from the AQUASTAT database for the reference period. They also used projections of the water demand per sector from (SHEN et al., 2010) which were incorporated into H08 hydrological model (Hanasaki et al., 2008) to obtain global scale gridded future projections of water demand for different SSP scenarios (Hanasaki et al., 2013). These projections were used in the present study to incorporate future changes in the water demand, per socio-economic scenario.

2.6.3. Indicators of adaptive capacity

The adaptive capacity refers to the ability of the society and the economy to cope with climate induced water availability variability and extremes. Adaptive capacity is measured in terms of resources availability i.e. human capital, financial capital and infrastructure, and the required institutional capital to utilize the former resources.

2.6.3.1. Economic resources available to adapt. The first indicator that was adopted is the gross domestic product (GDP) as it is expressed by the Purchasing Power Parity (PPP). GDP serves as a proxy of the available financial capital that can be utilized for adaptation actions. The GDP of the reference period were obtained from the World Bank data of International Institute for Applied Systems Analysis – IIASA database.[1] The same database provided GDP projections for the SSPs (Arnell et al., 2011a, 2011b; Moss et al., 2010) for the respective SWL periods listed in Table 1.

2.6.3.2. Law enforcement and human capital. Two indicators were considered for the inclusion of the institutional capital that can utilize adaptation measures. First, the law enforcement ability reflects a country's capability to plan and implement policies regarding water management and drought impact alleviation (Kaufmann et al., 2010). The data were obtained from the Worldwide Governance Indicators (WGI - www.govindicators.org). Human capital was the second indicator was the human capital described by the percent of highly educated workforce (Russo et al., 2012). Human capital in terms of educational level is important as it is highly related to the ability to manage information, in this case, related to water management and/or water policy application.

2.6.3.3. Level of natural or artificial freshwater storage capacity. A third pillar of adaptive capacity indicators is related to the natural and the artificial infrastructure that can serve for the mitigation of a climate related water scarcity issue. The most appropriate indicator is the ability to retain freshwater for use during a drought event. The indicator was expressed by two different indices, the extent of highly productive aquifers and inland waterbodies and the storage capacity of dams. In the former, the desalination capacity was also included as a source of artificially stored freshwater. For the derivation of the potential to natural freshwater storage capacity data from the IHME1500 v1.1 were obtained. This data is a state of the art result of digitization of the 25 map sheets of the International Hydrogeological Map of Europe at the scale of 1:1,500,000 (IHME1500) (Duscher et al., 2015). For the indicator of artificial freshwater storage capacity, information of the FAO geo-referenced dams' database was used (http://www.fao.org/nr/water/aquastat/dams/index.stm). Data for desalination and countries like Malta and Denmark was gathered from different sources.

[1] https://secure.iiasa.ac.at/web-apps/ene/SspDb/dsd?Action=htmlpage&page=about.

3. Results and discussion

3.1. Forcing variables

The domain of study is the European region. Fig. 1 shows the ensemble mean changes in precipitation (top panel) and temperature (bottom panel) and the corresponding agreement of the ensemble members on whether the examined variables increase in the projected time-slices. The results indicate that under +1.5 and +2 °C of global warming mean annual precipitation is expected to increase for most of the European region. Decreased precipitation is projected only for the Iberian Peninsula, southern Italy and southern Greece. Regarding model agreement, 80 to 100% of the models agree on the positive changes in projected precipitation. Model agreement is lower for the negative changes (60 to 80%). Precipitation projections for the +4 °C time-slice show decreasing trends over the Mediterranean region, including south Balkans and south France and positive changes for central and north Europe. The confidence on the projected changes is considerably increased at +4 °C, as model agreement is 80 to 100% for both the negative and positive signs of change. The direction of the change in precipitation remains unclear for a narrow zone that crosses central Europe, where projected changes are small (−5 to +5 mm/year) and model agreement the lowest (40 to 60%). Regarding temperature changes, due to the SWL concept for selecting time-periods, there is 100% model agreement on temperature increase for all the projected time-slices. Temperature increases are more intense at north-eastern Europe and the Mediterranean compared to the rest of the continent. For the +1.5 °C time-slice temperature increases over Europe range from +0.5 °C in the British Isles to up to +2 °C in the northern part of the Scandinavian peninsula. The +2 °C of global warming translates into an increase of up to +2 °C for the Mediterranean and east Europe and up to +4 °C for north Scandinavia. The +2 °C change signal results are consistent with those analyzed in (Vautard et al., 2014). For +4 °C of global warming, projections show increases in temperature over Europe that span from +2 to +4 °C for the least affected areas (central Europe, British Isles) and from +4 to +6 °C for the rest of the continent.

The results were also spatially aggregated for eight European sub-regions, proposed by Christensen and Christensen (2007), in order to assess climate change impacts at a regional level. The sub-regions of study are shown in Fig. 2. The relationship between precipitation and temperature changes at different SWLs for the eight examined European sub-regions is illustrated in Fig. 2. Spatially averaged values of precipitation and temperature changes at the projected time-slices are tabulated in Table ESM1 and Table ESM2 of the accompanying supplementary document, respectively. In Fig. 2 it can be observed that for higher levels of warming changes in precipitation and temperature are more intense for all the examined regions. Moreover, the variation of changes between the different regions is accentuated at higher warming levels. Under +1.5 °C of global warming, ensemble mean changes of precipitation and temperature are positive for all the regions and their spread over the x and y axis is small. Ensemble mean precipitation changes span from +1.91 mm/year (for the Iberian Peninsula) to +42.39 mm/year (for the Alps) and temperature changes fluctuate between +0.68 (for the British Isles) and +1.25 (for Scandinavia). The Iberian Peninsula, France and the Mediterranean show small increases in ensemble mean precipitation, which however is the result of averaging positive and negative changes of similar absolute magnitude. Generally, the range of the ensemble members' values is large and spans through negative and positive changes for four out of the eight sub-regions (IP, FR, MD and BI). At the +2 °C time-slice, the Iberian Peninsula is the only region where a negative change in ensemble mean precipitation is encountered, with half the models agreeing on the sign of the change. For France and Mediterranean ensemble mean changes in precipitation are positive, although 3 out of 6 and 4 out of 6 models respectively show decreasing trends. The regions where the smaller and larger changes and precipitation and temperature are found are the same with the +1.5 °C time-

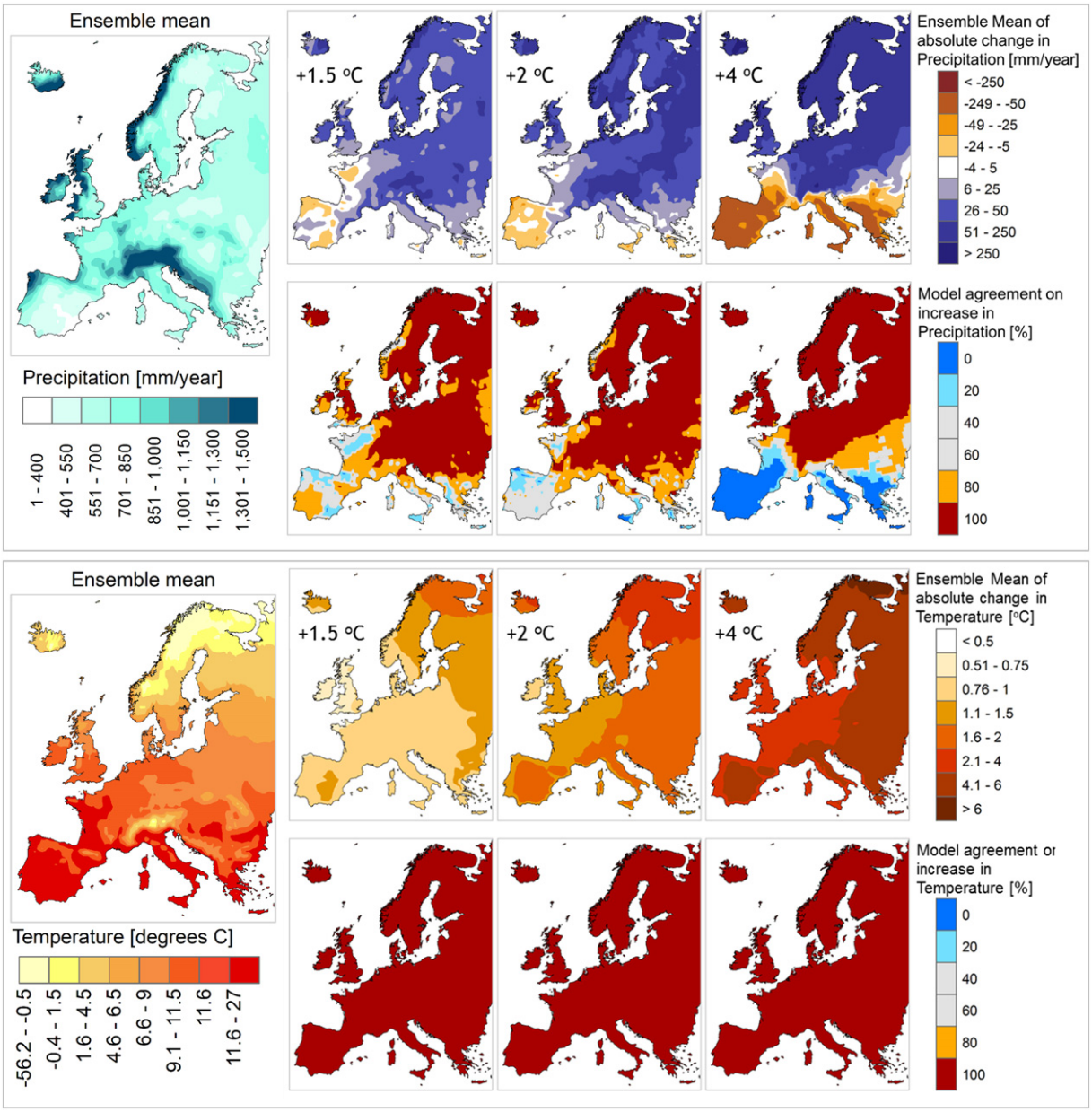

Fig. 1. Ensemble mean of precipitation and temperature for the baseline period (left), absolute changes in precipitation [mm/year] (top panel) and temperature [°C] (bottom panel) and corresponding model agreement towards the increase of precipitation and temperature in the projected time-slice (bottom row) for the three projected time-slices.

slice. Under +4 °C of global warming, reductions in ensemble mean precipitation are projected for France, the Mediterranean and the Iberian Peninsula and increases for the rest of the regions. The greatest ensemble mean reduction is found for the Iberian Peninsula (−80.56 mm/year). Scandinavia shows the largest increases in both precipitation (+145.98 mm/year) and temperature (+4.46 °C) while the smallest ensemble mean temperature increase is found for the British Isles. Detailed results for mean precipitation and temperature along with the anomalies of the individual ensemble members from the ensemble mean for the baseline period and the projected warming levels are illustrated in the first two figures (Figs. ESM1 & ESM2) of the accompanying electronic supplementary material.

3.2. Changes in runoff regime

Fig. 3 shows the ensemble mean of relative changes in mean annual runoff per SWL and the corresponding model agreement (top panel). Under +1.5 and +2 °C of warming, runoff production is projected to increase for the majority of the European land area, namely the north east half of the continent, the British Isles and even parts of the Mediterranean. Similar patterns of future runoff changes over Europe have been simulated under the high end RCP8.5 (Alfieri et al., 2015; Davie et al., 2013) and also even the under the moderate RCP4.5 scenario (Donnelly et al., 2017; Panagos et al., 2017) foreseeing important implications for water related issues. The projected runoff increases are larger at higher latitudes, especially at the +2 °C time-slice. The rest of the continent shows only minor variations in the mean annual runoff regime (−5 to +5%). 80 to 100% of the models agree on the projected increase of mean annual runoff while agreement is reduced (40 to 60%) for the areas where minor changes are encountered. At the +4 °C time-slice the positive changes in runoff production at the higher latitudes are intensified. Moreover, all models agree on the sign of the change in these regions. Reductions in mean annual runoff of up to −25% are projected for parts of the Mediterranean region, with 80 to 100% model agreement.

The projected relative changes in 10th percentile runoff production and the corresponding model agreement per SWL are illustrated in Fig.

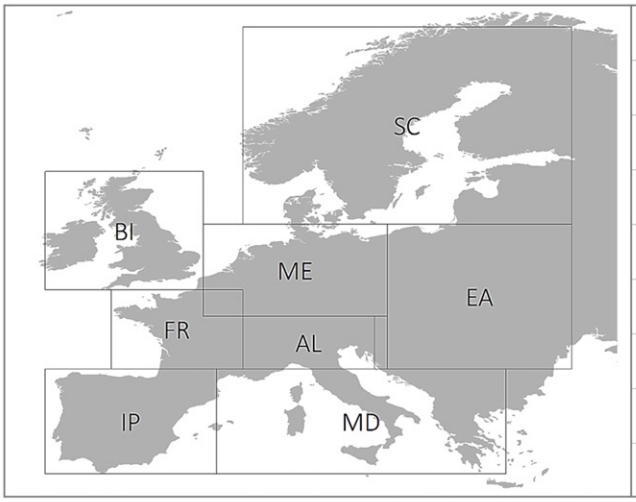

Region	Name
BI	British Isles
IP	Iberian Peninsula
FR	France
ME	Mid-Europe
SC	Scandinavia
AL	Alps
MD	Mediterranean
EA	Eastern Europe

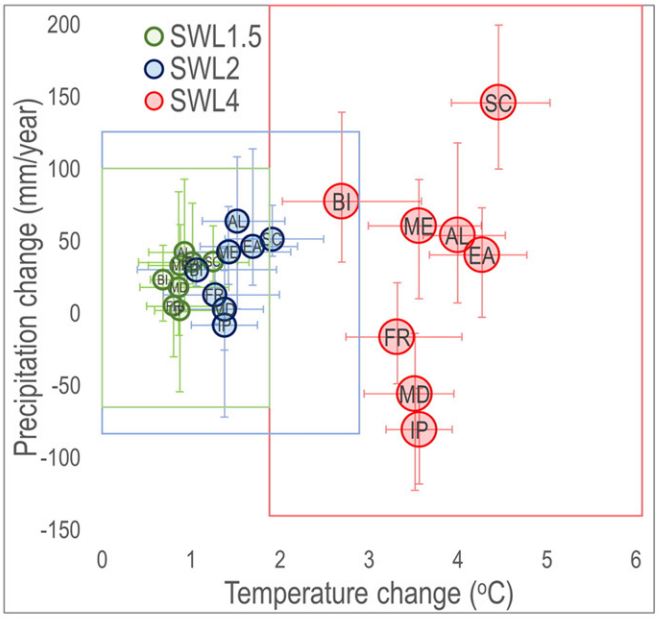

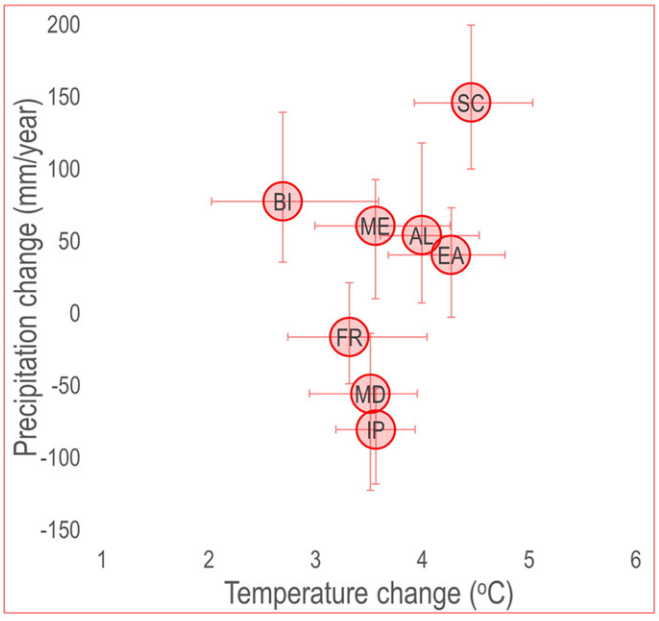

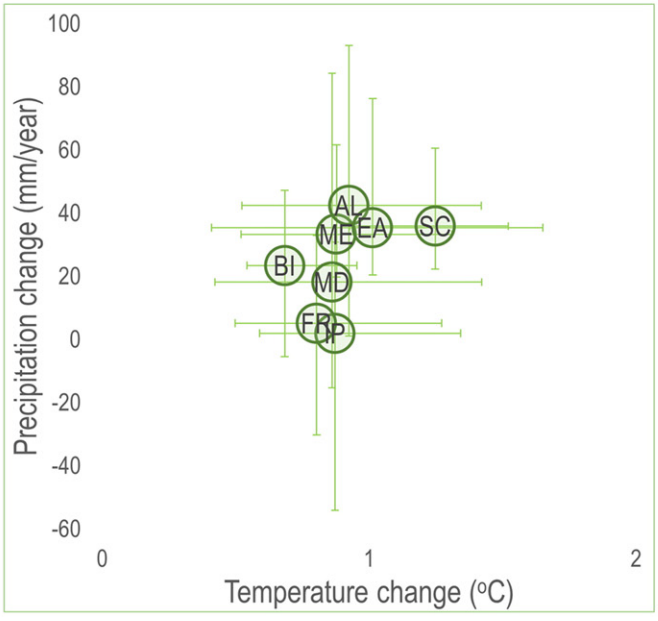

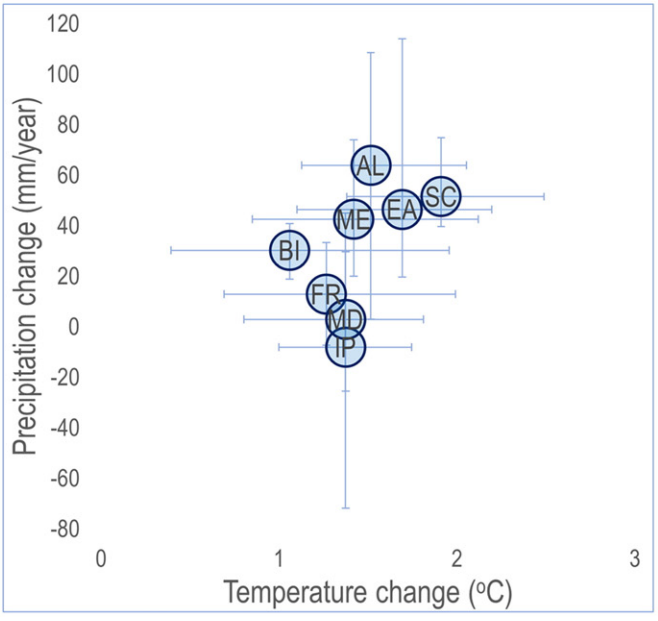

Fig. 2. Studied European sub-regions (Christensen and Christensen, 2007). Scatterplot of precipitation versus temperature changes per European region and per SWL. In the upper left panel all the SWLs are presented and in the rest panels the SWLS are demonstrated individually for clarity. Bars indicate the range of model projections for each parameter within each region.

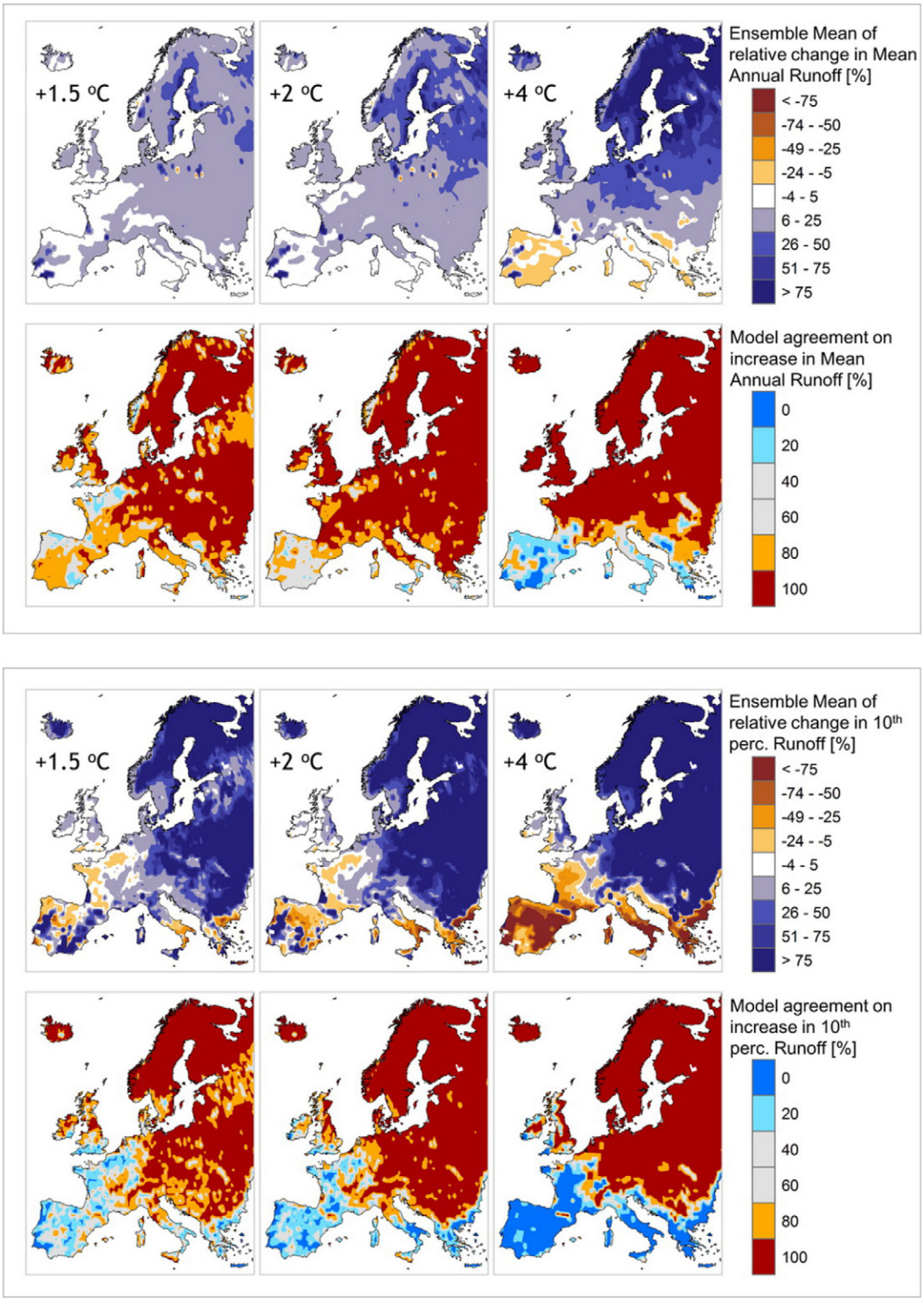

Fig. 3. Ensemble mean of relative changes in mean annual runoff (top panel) and in 10th percentile "low" runoff [mm/year] (bottom panel) and corresponding model agreement towards the increase of mean annual runoff and 10th percentile runoff in the projected time-slice for the three projected time-slices.

3 (bottom panel). Relative changes in 10th percentile runoff are exacerbated compared to changes in mean annual runoff. The response of 10th percentile runoff to global warming is very similar at +1.5 and +2 °C. Increases in 10th percentile runoff, with 80 to 100% model agreement, are projected for central, central east, north and north east Europe. With the same levels of agreement, reductions in 10th percentile runoff are projected for south Italy, Greece, regions in the west part of France and the north half of the Iberian Peninsula. Under +4 °C of global warming, reduced 10th percentile runoff is projected for all the Mediterranean countries, Portugal and west France, with 100% model agreement in the majority of the affected area. For the rest of Europe (the north east part of the continent and Iceland) 10th percentile runoff is projected to increase with 100% agreement between the models.

Spatially averaged values of ensemble mean changes in mean and 10th percentile runoff per sub-region and SWL are shown in Table ESM3 and ESM4, respectively, in the supplementary information file.

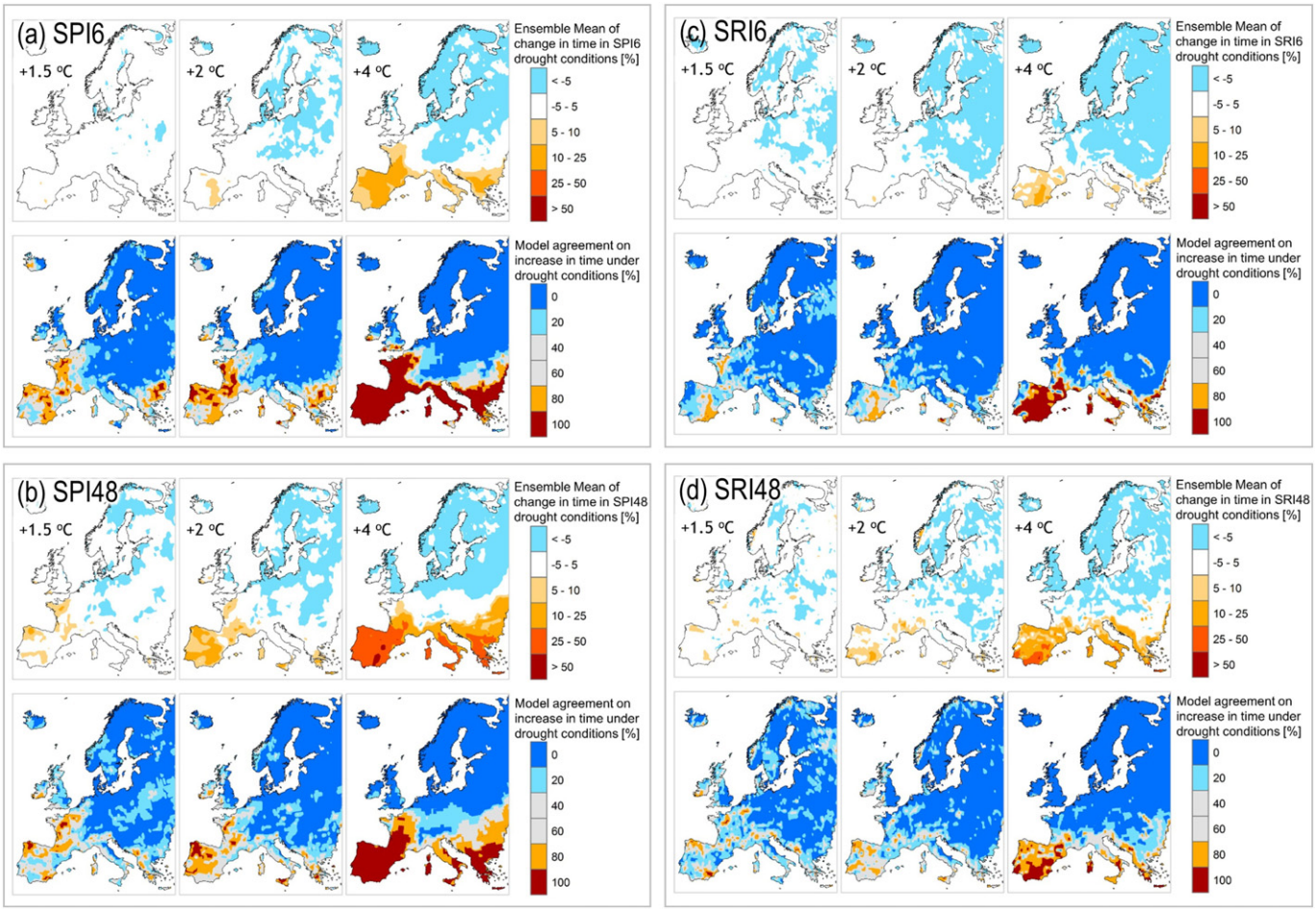

Fig. 4. Ensemble mean of change percent of time under drought conditions, described by the SPI-6, SPI-48, SRI-6 and SRI-48 drought indices [%] (top rows of each panel) and model agreement towards the increase in time under drought conditions (bottom rows) for the three projected time-slices.

Anomalies of the individual ensemble members from the ensemble mean annual runoff and 10th percentile runoff are included in the electronic supplementary material (Figures ESM3 & ESM4, respectively).

3.3. Drought indices

Fig. 4a shows the projected changes in percent of time per SWL that drought conditions prevail in the European area, as defined by the SPI-6 and SPI-48 drought indices respectively. Regarding the results on the short-term drought index SPI-6, in Fig. 4a it can be observed that under +1.5 °C of global warming there is no significant increase in time under drought conditions. At the +2 °C time-slice, an increase in drought conditions' duration of 5 to 10% is projected for a west part of the Iberian Peninsula. The time under drought conditions is notably increased at the +4 °C SWL (5 to 25%) for the Mediterranean region. In contrast, the time extent of droughts is expected to decrease for north Europe and parts of central Europe. It is worth noting that at the +4 °C time-slice, both the projected increases and decreases in time under droughts in the south and the north parts of Europe respectively are supported by 100% of the models.

The results on the long-term drought index SPI-48, show a slightly exacerbated response to climate change compared to short-term drought results (Fig. 4b). At +1.5 °C, increases in drought duration are projected for parts of the Iberian Peninsula and west France. At +2 °C, the former increases expand to cover the whole Iberian Peninsula, in addition to west France and Greece. The model agreement for these changes ranges from 60 to 100%. Under +4 °C of global warming, increases in drought duration ranging from 25 to >50% are projected for the Mediterranean with 100% model agreement on the sign of the change. In the zone north of the Mediterranean time under drought conditions is projected to increase from 5 to 25%, with a one tier reduction on the agreement scale (80% for most of the affected area). For the north part of the continent all models agree on a decrease in time under long-term drought conditions.

Changes in short- and long-term drought conditions, expressed by the SRI index, per SWL are shown in Fig. 4c and d respectively. The climate change impacts projected for droughts by the SRI index are less dramatic compared to the results of the SPI index. This can be justified by the fact that runoff is a component of the water cycle that, apart from precipitation and evapotranspiration, is also affected by soil moisture. Thus the SRI index will have a slower and more moderate response to a long-term deficit in precipitation compared to SPI. The results of the short-term drought index SRI-6, suggest no increases in total drought duration under +1.5 and +2 °C of warming. At +4 °C, increases of 5 to 25% in time under drought conditions are projected for the east part of the Iberian Peninsula and some smaller areas in Italy and Greece, with 100% model agreement. Again, changes are more intense for the long-term drought conditions. Under +1.5 °C of global warming, duration of drought conditions defined by SRI-48 is not expected to change significantly over Europe. At the +2 °C time-slice, projected increases of 5 to 25% in drought duration are identified for parts of the Iberian Peninsula (with 80% model agreement). Increases are also found for south France, but the model agreement on increase in drought duration in this area is weak. At the +4 °C time-slice, time under drought conditions

is projected to increase by 25 to 50% in the south Mediterranean regions and by 5 to 25% in the rest of the Mediterranean. In the most affected by climate change south part of the Mediterranean, all models agree towards the increase in drought duration. For the central and north part of the Mediterranean, model agreement is lower (80% at the majority of the region and 60% in some regions, e.g. in north Italy).

3.4. Future estimates of exposure, sensitivity and adaptive capacity

3.4.1. Exposure

The relative exposure to freshwater availability was derived from the combined information of the mean and low annual runoff production, SPI and SRI indices, spatially aggregated at NUTS2 level over Europe, for the reference and the projected periods of the three SWLs (Fig. ESM5 in the electronic supplementary). The relatively high exposure of middle-east and north-eastern Europe is projected to alleviate by the increasingly highest runoff production of the subsequent SWL periods. The opposite is expected for the southern part of Europe. The range of the projected relative exposure to freshwater availability as derived from the hydrological simulation of the six model ensemble indicates reduced model agreement with higher warming. This wider range of modeled exposure is more pronounced for several regions, like for example the Iberian Peninsula, for which a diverse signal of drier (r1, r4, r6) or wetter (r2, r3, r5) response is foreseen. Fig. ESM6 is a similar representation of Fig. ESM5 on the relative exposure but for low flows at the spatial level of NUTS2 local administrative boundaries. The signal of change for the relative exposure to low flows is similar to the corresponding of the mean annual runoff production but even more clear and robust in terms of model agreement.

As shown in Fig. ESM7 Spain and Portugal, Southern Italy and mainland Greece, the Scandinavian Peninsula, Great Britain and Ireland as well as central Europe are relatively more highly exposed areas to short term hydrological drought. The severity of exposure is even more pronounced for higher levels of warming over southern Europe while the opposite is projected for northern Europe. Especially for SWL4 the Iberian and the Scandinavian Peninsulas are expected to be in a state of higher and lower exposure, respectively, in their entirety. The relatively Pan-European moderate exposure to long term meteorological droughts (Fig. ESM8) of the recent past period is attenuated for central and northern Europe and more severe for southern Europe. There is an overall considerable variation of the projected exposure to long term meteorological drought between the models for the SWLs of 1.5 and 2°, while for the higher level of 4 degrees of warming, models agree on the increased exposure over the northern Mediterranean region. For the description of short (Fig. ESM9) and long term (Fig. ESM10) hydrological drought, SRI was employed in order to provide additional information on exposure by capturing hydrological processes and associated droughts which cannot be described by SPI (meteorological drought). For example while northwestern Spain and north Portugal are classified as highly exposed to short term meteorological droughts the opposite is depicted with the use of SRI for hydrological drought. Thus, the use of two temporal scales (6 and 48 months) and also the use of SRI additional to SPI complements the overall concept of drought exposure.

Figure ESM11 illustrates the full range of model projected relative overall exposure to freshwater availability, as derived through the combination of the exposure indicators, at NUTS2 level for the baseline and the SWL periods following high end climate change (RCP8.5). The indicators of average water availability, low flows and extreme events relevant to water availability (short and long term droughts) were combined with equal weighting (Table 2). The increase in precipitation for most of the European region, despite the higher temperatures of the SWLs, is the major driver for a consequent increase in runoff production. As a result, the relative overall exposure is projected to decrease for the majority of the European land area except the Mediterranean.

3.4.2. Sensitivity

In the present analysis, the population density of year 2014 was considered for each NUTS2 area (population per square kilometre) and served as the reference population density of the baseline period (Fig. ESM12). The respective data were retrieved from ESRI (Michael Bauer Research GmbH). Although abrupt changes are not expected, some regions may face significant changes in their population, leading to increased water stress (Kovats et al., 2014). Here, the change in the population density was estimated for each SSP scenario and SWL, for each NUTS2 area. The projections were obtained from IASSA (KC and Lutz, 2014) for the different SSPs at the corresponding year of passing the SWL1.5, SWL2 or SWL4 (Fig. ESM12). Fig. ESM13 presents a collective picture of the evolution of European population according to three socio-economic scenarios (SSP2, SSP3 and SSP5) for the SWLs crossing years for the range of climate model projections used in the present study.

The sensitivity of agricultural areas was expressed by the extent of irrigation as the percent of the cultivated area that is irrigated, at NUTS2 level. Fraction of Irrigated area was obtained from FAO's AQUASTAT website and is shown in Fig. ESM14.

Fig ESM15 shows the spatial distribution of total water demand for the crossing time of SWL1.5, SWL2 and SWL4 according to different SSPs over Europe, in NUTS2 level. Fig. ESM16 also illustrates the temporal evolution of water use scenarios at Pan-European level according to three socio-economic pathways (SSP2, SSP3 and SSP5) for the SWLs crossing years of each climate model for the full range of climate projections. Both SSP5 and SSP3 of convectional development and fragmentation, correspondingly are considered of high growth in terms of irrigated area and crop intensity while SSP2, the middle road, is regarded as medium growth. In terms of water use efficiency (mainly for irrigation), SSP5 represents a situation of high efficiency, SSP2 of medium and SSP3 of low efficiency, as illustrated in Fig. ESM16.

The sensitivity indicators (Table 2) where equally weighted for the estimation of the sensitivity index. High population density areas like Great Britain, central European countries and capital regions contribute to the increase of overall sensitivity. Increase in projected population according to the different socio-economic pathways (and especially for SSP5) are enhancing the sensitivity. Highly irrigation dependent areas like the Mediterranean countries, Balkan area and the Netherlands result to higher overall sensitivity. The same is true for the total water demand. On the other hand, the combination of the indicators of population density and total water demand compensates the total sensitivity of the future. For example, the increase in sensitivity due to population increase according to SSP5 is counterbalanced by the higher water use efficiency assumed for this pathway. Finally, Figure ESM17 illustrates the full range of model projected relative overall exposure to freshwater availability, as derived through the combination of the exposure indicators, at NUTS2 level for the baseline and the SWL periods following high end climate change (RCP8.5).

3.4.3. Adaptive capacity

Western European countries have and are foreseen to “afford” (from a GDP perspective) higher adaptation activities across all SSPs. This diversity between the European countries is more pronounced at higher levels of warming. Fig. ESM18 shows country level GDP per capita for the reference period and the defined combinations of SWLs and SSPs. Fig. ESM19 depicts the European GDP-PPP according to three socio-economic scenarios (SSP2, SSP3 and SSP5) for the SWLs crossing years for a range of climate model projections.

Northern and western European countries show an adaptation advantage in terms of institutional capital. This is related to the ability of law enforcements, and more specifically for the present study the governmental ability, of formulation and implementation of policies and regulations of the water sector. Thus, countries like Finland, Norway, Denmark and Sweden are classified as more capable compared to several countries in the wider Balkan region (Fig. ESM20). A similar spatial

Fig. 5. Country level aggregated exposure (left), sensitivity (middle) and adaptive capacity (right) for the baseline and the SWLs. Exposure is presented as error bars which represent the mean and the range of the ensemble's exposure values for each country.

pattern is presented for the adaptive capacity related to the human capital in terms of water management and policy application (Fig. ESM21). It is important to note that countries with potential higher exposure to future freshwater stress (Fig. ESM7 to Fig. ESM10) have the lower adaptation capacity coming from their human capital.

Central Europe is also benefited from the presence of relative high aquifer production and inland waterbodies. For countries (EU28) like Estonia, the Netherlands and Slovenia the extent of highly productive aquifers and inland waterbodies is over 50% of their total land area (Fig ESM22). On the other hand for Malta, Portugal, Ireland, Czech Republic, Finland, Sweden and Cyprus this extent is <10%. Regarding the adaptive capacity related to storage of dams and desalination potential Sweden, Denmark, Spain, Portugal and Bulgaria are ranked with the higher scores among the EU28 countries, while Finland, Belgium, Slovenia and Hungary present the lower level of artificial freshwater storage (Fig. ESM23).

Finally, Fig. ESM24 is the result of the combination of the aforementioned adaptive capacity indicators, illustrating the overall adaptive capacity related to freshwater shortage at NUTS2 level for the baseline and the SWL periods following high end climate change (RCP8.5) for a range of model projections and plausible SSP combinations. Higher GDP per capita and human capital, as well as more effective governance for most of the western and north European countries result to a higher overall adaptive capacity related to freshwater shortage of these regions. Natural and artificial storage potential plays also an important role in shaping the total adaptive capacity. United Kingdom, the Netherlands and France are ranked as the EU28 countries with the higher adaptive capacity and

on the contrary, Croatia, Malta and Bulgaria the least adaptive, for all the examined states of global warming level and socio-economic status.

3.5. Vulnerability profiles and patterns under different adaptation pathways

Country level aggregates of total exposure, sensitivity and adaptive capacity per SWL and SSP are shown in Fig. 5. For the northern European countries, exposure is decreased with the progressing of warming. In contrast, southern and Mediterranean countries face increased exposure compared to baseline as higher SWLs are reached. Cyprus and Malta are the more exposed countries across all levels of warming. Spain, Portugal and Greece complement the highest exposure ranking for the 2 °C and 4 °C levels of warming. Although the average range of projected exposure is of the same range for the three warming levels, there are remarkable changes at country level. For example Cyprus is projected to be the most exposed country in terms of freshwater stress for all the examined warming levels. At the same time the range of exposure for Cyprus at the 1.5 °C warming is ranked as the second higher. This range is reduced for the subsequent warming levels resulting to one of the lowest for the 4 °C level of warming. This indicates a higher

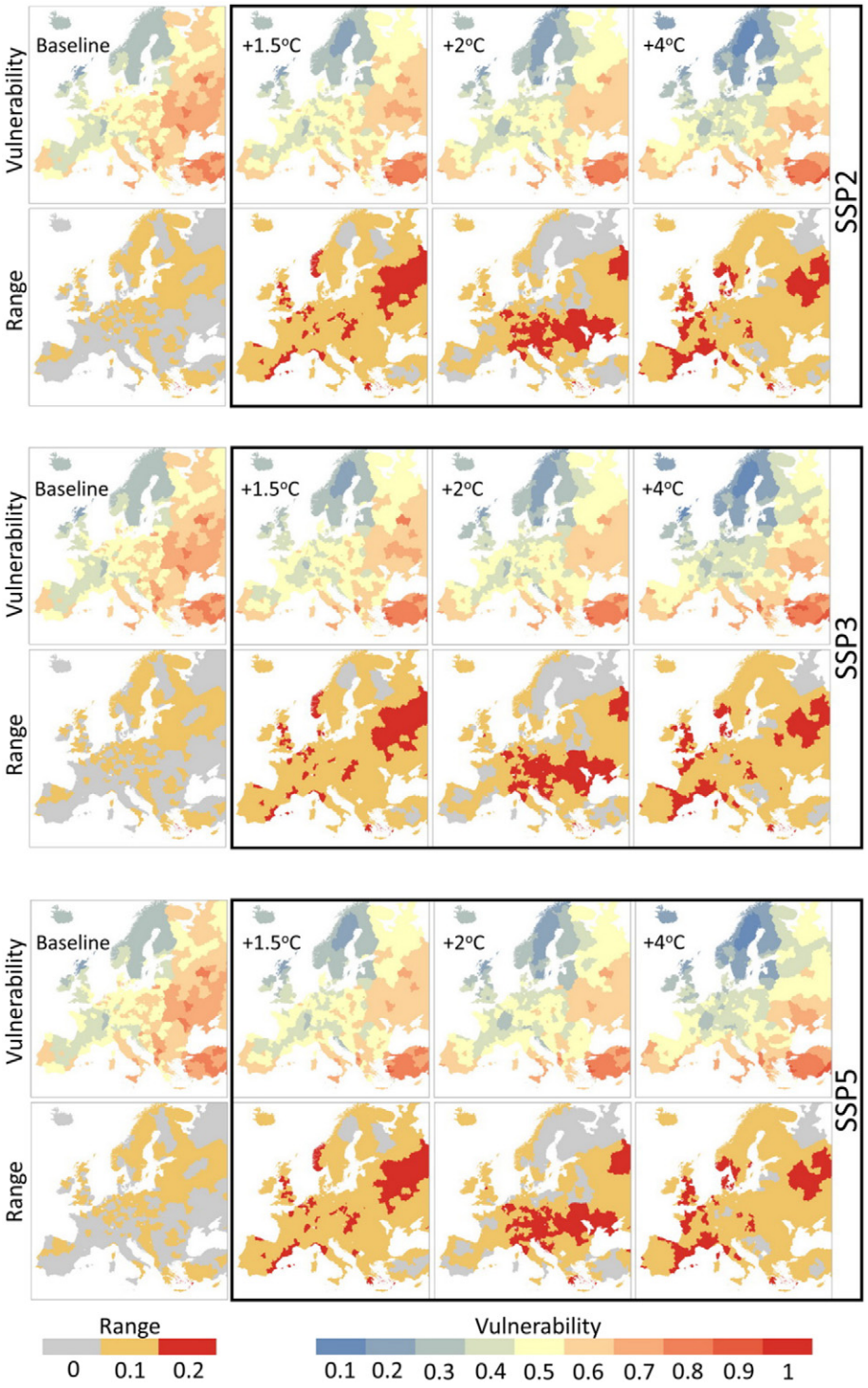

Fig. 6. Relative overall vulnerability to freshwater availability at NUTS2 level for the baseline and the SWL periods following high end climate change (RCP8.5) according to different SSPs. Lower panels illustrate the multi model range of relative vulnerability.

consensus in modeled exposure for Cyprus as global warming increases. Looking deeper into the sub-indices of exposure, most of this variability (for Cyprus) is coming from the indicator of short term meteorological droughts (SPI6) and this is probably due to the different intra-annual precipitation variability signals from the different climate model simulations driven by different SST patterns. This example of thorough analysis can be performed for every EU28 country (or event in more detail at NUTS2 level) providing the ability to identify specific sources of exposure (changes in mean or low flows, changes in short or long term meteorological and hydrological drought).

Italy and Netherlands are the most freshwater "sensitive" EU28 countries for all the examined levels of warming and corresponding socioeconomic scenarios, according to our approach. This high sensitivity for Italy stems from its high dependency of agriculture on irrigation and the relatively high water demand in total (domestic, industrial, and agricultural sectors) and less by the density of population, which is relatively average within the EU28 level. Netherlands is classified at a similar state having also higher sensitivity in terms of population density. On the other hand countries with low sensitivity are Latvia, Estonia, Sweden and in general north and northeastern European countries.

United Kingdom is projected to have the highest adaptive capacity across all SSPs and warming levels mostly due to the high levels of human capital and policy enforcement combined with the higher GDP. Netherlands is also rated just after the UK with a high adaptive potential, with high ratings for all adaptation sub-indices. Germany, France, Sweden, Slovenia and Finland complement the group of EU28 countries with relatively higher adaptation potential against freshwater shortages. Croatia, Malta, Bulgaria, Hungary, and Czech Republic are classified as countries with lower resources for adaptation. In general, the highest adaptive capacity is reported for countries of central and north Europe. Sensitivity and adaptive capacity do not show notable differences for different SWLs. This may, to some degree, stem from the spatial aggregation of the information on the NUTS2 level to the country level (NUTS0).

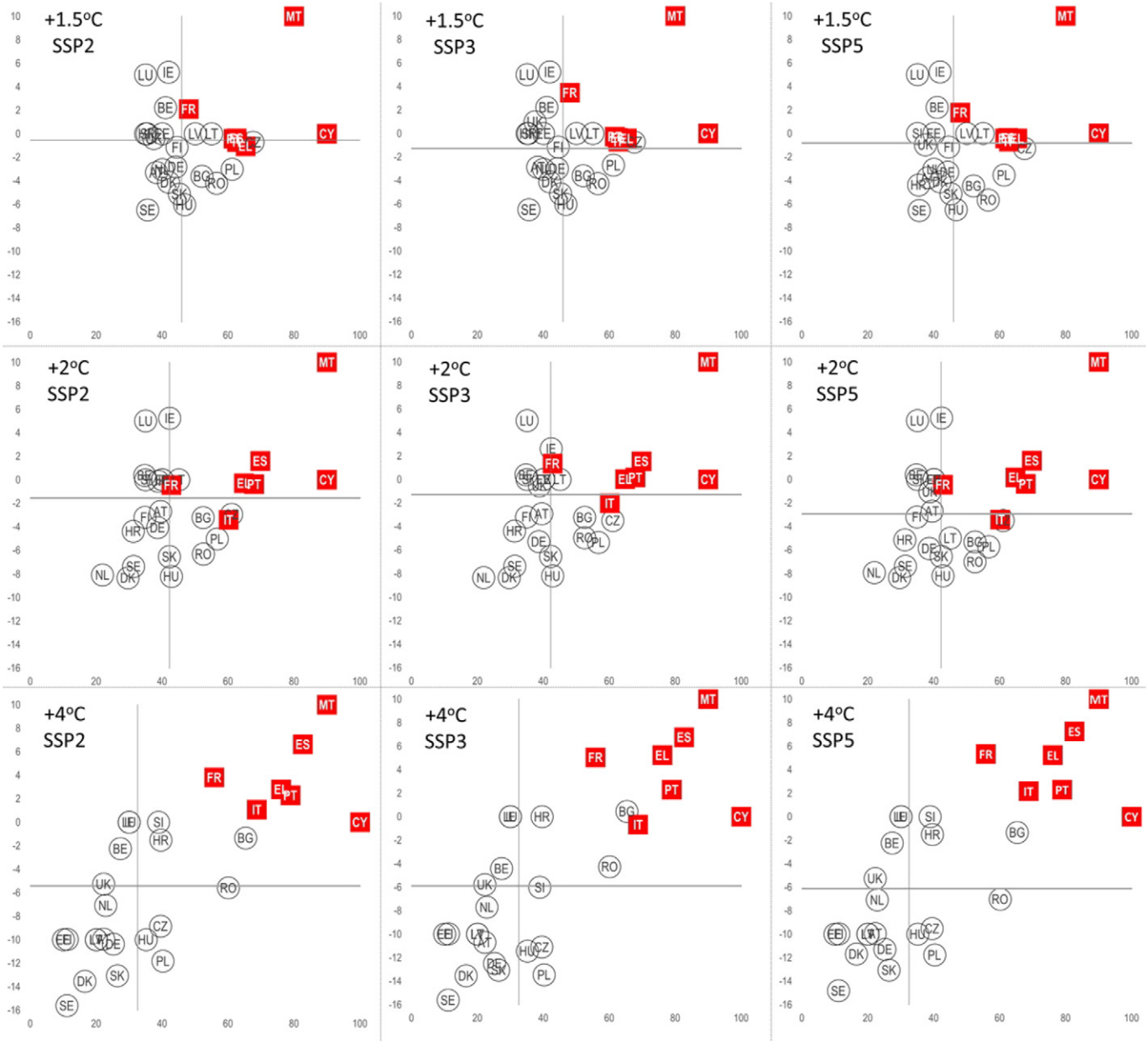

Fig. 7. Change in relative overall vulnerability from baseline against relative exposure for the EU-28 countries. Mediterranean countries are marked with red color. Positions of the x and y axis correspond to the median value of change in vulnerability and exposure respectively. The median is derived from the 28 values presented in the scatterplots. Scatterplots are presented for all the SWLs and SSPs combinations.

The combination of exposure, sensitivity and adaptive capacity leads to vulnerability profiles at NUTS2 level for the European region, for the baseline period and the considered SWLs, for the SSPs that correspond to the RCP8.5 emission pathway (Fig. 6). An observation common for all the considered time-slices is that northern countries show the lowest vulnerability values and Mediterranean countries along with east European countries are the most vulnerable regions. There are only marginal differences between the vulnerability patterns of the baseline period and the SWLs. These concern decreases in vulnerability for north and central Europe and vulnerability increases in the Mediterranean. Multi-model vulnerability range (also shown in Fig. 6) is relatively small (0 to 0.2). The highest uncertainty in the vulnerability patterns is reported for the central-east European region across all the considered SWLs and for central Europe at SWL2.

The relationship between changes in vulnerability with respect to baseline conditions and exposure for the EU-28 countries is illustrated with the scatterplots shown in Fig. 7. The first quartile corresponds to both increased vulnerability and high exposure. Respectively, the third quartile corresponds to decreased vulnerability and low exposure. Thus countries whose values fall in the first quartile are the most endangered by global warming while countries of the third quartile are the safest with respect to climate change risks. For each SWL, the relationship of vulnerability change and exposure does not fluctuate between the three SSPs. In contrast, as higher SWLs are examined, the distinction between "endangered" and "safe" countries becomes more pronounced. At SWL4, the Mediterranean and east European countries are projected to experience both increased vulnerability and high exposure while the rest of the EU-28 countries are "safer" due to their low exposure and decreased vulnerability. A few clear conclusions emerge from the country level aggregates of Fig. 7. Relative exposure is expected to increase compared to the recent past only for Malta and Cyprus at a 1.5 °C and 2 °C global fast warming states, while at the +4 °C France, Portugal, Spain, Italy, Greece and Bulgaria are entering the higher exposure list. The rest of the EU28 countries are foreseen to have a decreased or similar level of exposure to freshwater stress. When comparing the changes in vulnerability for the various SSPs and warming levels, the outcomes of this framework indicate that pan-European freshwater vulnerability is probably expected to decrease on average. The largest decrease is associated with SSP5 although the same scenario foresees the largest increase of vulnerability for the Mediterranean countries. SSP5 is related to a road of convectional development (O'Neill et al., 2015) leaving room to high adaptation potential due to economic growth and efficiently water management due to high technological progress and intensive agricultural land management. SSP2 follows in terms of vulnerability reduction for the SWLs of +1.5 °C and +2 °C as "a middle of the road" scenario, following the recent trends of socio-economic conditions, in contrast with SSP3 that is related to a more fragmented world difficult to mitigate and adapt. SSP3 results to a lower vulnerability compared to SSP2 only for the +4 °C level probably due to the increase in the economic resources, but for specific countries of the EU28, of a potentially highly fragmented Europe.

4. Conclusions

This study examines the freshwater vulnerability under a high-end climate change scenario (RCP8.5) with the use of a vulnerability index at a pan European scale. The vulnerability framework was based on the most relevant indicators related to water availability and stress with the best available spatial resolution (NUTS level 2). The approach was applied for three levels of global warming (1.5 °C, 2 °C and 4 °C) and examining various adaptation tiers, corresponding to specific socioeconomic pathways (SSP2, SSP3 and SSP5), thus covering a wide range of possible "water futures". Several studies have been performed addressing water vulnerability under climate change impacts at the European or regional level, without adhering with the RCP/SSP framework. Dunford et al. (2015) for example examined the water exploitation vulnerability for a set of socio-economic and climate scenarios using indicators of coping capacity, mapping a vulnerable-hard to cope European south. At the regional level several assessments use case specific scenarios of socioeconomic development (Collet et al., 2015; Grouillet et al., 2015; Koutroulis et al., 2013; Stigter et al., 2017) that could be easily adjusted to the RCP/SSP framework. Other studies are focusing on the examination on drought assessment based on hydrological impacts not considering the future socioeconomic developments (Arnell et al., 2016; Roudier et al., 2016). In contrast to most of these studies, dealing with future estimates of water availability and stress, our approach combines specific levels of socioeconomic development elaborating the harmonized SSP framework, which combined with specific warming levels, provides important information on the ability to adapt. Thus, the use of a unified RCP/SSP framework allows for a consistent examination of the influence of the level of adaptation challenges to the freshwater vulnerability (Hanasaki et al., 2013; Koutroulis et al., 2016; Mouratiadou et al., 2016; Veldkamp et al., 2016; Wada et al., 2016).

Country level aggregates indicate that Mediterranean countries are the most exposed and there is a high modeling consensus on increased vulnerability for these countries as global warming increases. It is also important to note that countries with potential higher exposure to future freshwater stress have the lower adaptation capacity stemming from the level of the human capital. These countries have to develop and invest in appropriate strategies in order to advance education for the sake of sustainability and adaptation to a potential drier future. Northern European countries are the least vulnerable due to lower exposure (wetter projections) and high adaptive capacity (in terms of economic resources available to adapt, law enforcement and human capital). Along with the major findings, there are also several limitations of the applied methodology that have to be highlighted. National level aggregates have to be interpreted with caution since local spatial variability is smoothed, especially for large countries. Another issue is the weighting of the relevant indicators. Equal weighting has been used in the current approach and potential future research could elaborate on different and more sophisticated weighting schemes. The relationships between the various indicators and their potential interactions are a field which could be further investigated.

The value of the current approach is the description of freshwater vulnerability with a single index and at the same time the depth of the underlying information. Looking deeper into the information provided by the basic indices and their sub-indices, one can trace the sources of high or low vulnerability and whether this stems from high or low exposure, sensitivity or adaptive capacity. This information can be identified at a NUTS2 spatial classification level which corresponds to the basic regions for the application of regional policies, making this approach extremely useful for supporting regional level policy making and implementation and strategic planning against future freshwater stress.

Acknowledgements

The research leading to these results has received funding from the European Union Seventh Framework Programme FP7/2007-2013 under grant agreement no 603864 (HELIX: High-End cLimate Impacts and eXtremes; www.helixclimate.eu). The EC-EARTH3-HR simulations were performed on resources provided by the Swedish National Infrastructure for Computing (SNIC) at PDC.

Appendix A. Supplementary data

Supplementary data to this article can be found online at http://dx.doi.org/10.1016/j.scitotenv.2017.09.074.

References

Alcamo, J., Acosta-Michlik, L., Carius, A., Eierdanz, F., Klein, R., Krömker, D., Tänzler, D., 2008. A new approach to quantifying and comparing vulnerability to drought. Reg. Environ. Chang. 8, 137–149.

Alfieri, L., Burek, P., Feyen, L., Forzieri, G., 2015. Global warming increases the frequency of river floods in Europe. Hydrol. Earth Syst. Sci. 19:2247–2260. http://dx.doi.org/10.5194/hess-19-2247-2015.

Alfieri, L., Bisselink, B., Dottori, F., Naumann, G., de Roo, A., Salamon, P., Wyser, K., Feyen, L., 2017. Global projections of river flood risk in a warmer world. Earth's Futur. 5: 171–182. http://dx.doi.org/10.1002/2016EF000485.

Arnell, N.W., van Vuuren, D.P., Isaac, M., 2011a. The implications of climate policy for the impacts of climate change on global water resources. Glob. Environ. Chang. 21, 592–603.

Arnell, N.W., van Vuuren, D.P., Isaac, M., 2011b. The implications of climate policy for the impacts of climate change on global water resources. Glob. Environ. Chang. 21: 592–603. http://dx.doi.org/10.1016/j.gloenvcha.2011.01.015.

Arnell, N.W., Brown, S., Gosling, S.N., Gottschalk, P., Hinkel, J., Huntingford, C., Lloyd-Hughes, B., Lowe, J.A., Nicholls, R.J., Osborn, T.J., Osborne, T.M., Rose, G.A., Smith, P., Wheeler, T.R., Zelazowski, P., 2016. The impacts of climate change across the globe: a multi-sectoral assessment. Clim. Chang. 134:457–474. http://dx.doi.org/10.1007/s10584-014-1281-2.

Best, M.J., Pryor, M., Clark, D.B., Rooney, G.G., Essery, R.L.H., Ménard, C.B., Edwards, J.M., Hendry, M.a., Porson, A., Gedney, N., Mercado, L.M., Sitch, S., Blyth, E., Boucher, O., Cox, P.M., Grimmond, C.S.B., Harding, R.J., 2011. The Joint UK Land Environment Simulator (JULES), model description – part 1: energy and water fluxes. Geosci. Model Dev. 4:677–699. http://dx.doi.org/10.5194/gmd-4-677-2011.

Birkmann, J., Cardona, O.D., Carreño, M.L., Barbat, A.H., Pelling, M., Schneiderbauer, S., Kienberger, S., Keiler, M., Alexander, D.E., Zeil, P., 2014. Theoretical and conceptual framework for the assessment of vulnerability to natural hazards and climate change in Europe1. Assessment of Vulnerability to Natural Hazards: A European Perspective, p. 1.

Blauhut, V., Gudmundsson, L., Stahl, K., G, A., al, A.L. et, Beguería S, V.-S.S.M. and A.-M.M., E, B., A, D., EC, EC, EC, EEA, EEA, EEA, Commission, E., Fu X, S.M.T.Z.D.Z. and W.J., Gudmundsson L, R.F.C. and S.S.I., G, H., E, H.J.F., al, H.M.R. et, Iglesias A, C.A.W.D.A.G.L. and C.F. (ed), IPCC, IPCC, J, J.A., al, K.C.A. et, Knutson C, H.M. and P.T., al, K.M. et, R, K., al, L.-M.J.I. et, al, L.-L.J. et, E, M.S.J. and G.N., McKee T B, D.N.J. and K.J., al, N.G. et, V, P., Sheffield J, W.E.F. and R.M.L., al, S.J. et, Sreedhar G, N.R. and B. V, Stagge J H, T.L.M.K.I.S.K. and V.L.A., al, S.J.H. et, Stagge J H, T.L.M.G.L.V.L.A.F. and S.K., Stagge J H, K.I.T.L.M. and S.K., al, S.K. et, al, V.A.J. et, B, V.W.N. and R., al, V.-S.S.M. et, Vicente-Serrano S M, B.S. and L.-M.J.I., Wang Q, W.J.L.T.H.B.W.Z.L.M. and L.D., WHO, H, W.D.A. and G.M., Wilhite D A, S.M.D. and H.M.J., S, W.D., al, Z.A. et, al, Z.E. et, 2015. Towards pan-European drought risk maps: quantifying the link between drought indices and reported drought impacts. Environ. Res. Lett. 10:14008. http://dx.doi.org/10.1088/1748-9326/10/1/014008.

Blauhut, V., Stahl, K., Stagge, J.H., Tallaksen, L.M., De Stefano, L., Vogt, J., 2016. Estimating drought risk across Europe from reported drought impacts, drought indices, and vulnerability factors. Hydrol. Earth Syst. Sci. 20:2779–2800. http://dx.doi.org/10.5194/hess-20-2779-2016.

Brooks, N., Neil Adger, W., Mick Kelly, P., 2005. The determinants of vulnerability and adaptive capacity at the national level and the implications for adaptation. Glob. Environ. Chang. 15:151–163. http://dx.doi.org/10.1016/j.gloenvcha.2004.12.006.

Carrão, H., Naumann, G., Barbosa, P., 2016. Mapping global patterns of drought risk: an empirical framework based on sub-national estimates of hazard, exposure and vulnerability. Glob. Environ. Chang. 39:108–124. http://dx.doi.org/10.1016/j.gloenvcha.2016.04.012.

Chadburn, S., Burke, E., Essery, R., Boike, J., Langer, M., Heikenfeld, M., Cox, P., Friedlingstein, P., 2015. An improved representation of physical permafrost dynamics in the JULES land-surface model. Geosci. Model Dev. 8:1493–1508. http://dx.doi.org/10.5194/gmd-8-1493-2015.

Christensen, H.J., Christensen, B.O., 2007. A summary of the PRUDENCE model projections of changes in European climate by the end of this century. Clim. Res. 81:7–30. http://dx.doi.org/10.1007/s10584-006-9210-7.

Clark, D.B., Mercado, L.M., Sitch, S., Jones, C.D., Gedney, N., Best, M.J., Pryor, M., Rooney, G.G., Essery, R.L.H., Blyth, E., Boucher, O., Harding, R.J., Huntingford, C., Cox, P.M., 2011. The Joint UK Land Environment Simulator (JULES), model description – part 2: carbon fluxes and vegetation dynamics. Geosci. Model Dev. 4:701–722. http://dx.doi.org/10.5194/gmd-4-701-2011.

Collet, L., Ruelland, D., Estupina, V.B., Dezetter, A., Servat, E., 2015. Water supply sustainability and adaptation strategies under anthropogenic and climatic changes of a meso-scale Mediterranean catchment. Sci. Total Environ. 536:589–602. http://dx.doi.org/10.1016/j.scitotenv.2015.07.093.

Cutter, S.L., Finch, C., 2008. Temporal and spatial changes in social vulnerability to natural hazards. Proc. Natl. Acad. Sci. 105:2301–2306. http://dx.doi.org/10.1073/pnas.0710375105.

Davie, J.C.S., Falloon, P.D., Kahana, R., Dankers, R., Betts, R., Portmann, F.T., Wisser, D., Clark, D.B., Ito, A., Masaki, Y., Nishina, K., Fekete, B., Tessler, Z., Wada, Y., Liu, X., Tang, Q., Hagemann, S., Stacke, T., Pavlick, R., Schaphoff, S., Gosling, S.N., Franssen, W., Arnell, N., 2013. Comparing projections of future changes in runoff from hydrological and biome models in ISI-MIP. Earth Syst. Dynam. 4:359–374. http://dx.doi.org/10.5194/esd-4-359-2013.

Donnelly, C., Greuell, W., Andersson, J., Gerten, D., Pisacane, G., Roudier, P., Ludwig, F., 2017. Impacts of climate change on European hydrology at 1.5, 2 and 3 degrees mean global warming above preindustrial level. Climate Change http://dx.doi.org/10.1007/s10584-017-1971-7.

Dubrovsky, M., Svoboda, M.D., Trnka, M., Hayes, M.J., Wilhite, D.A., Zalud, Z., Hlavinka, P., 2009. Application of relative drought indices in assessing climate-change impacts on drought conditions in Czechia. Theor. Appl. Climatol. 96:155–171. http://dx.doi.org/10.1007/s00704-008-0020-x.

Dunford, R., Harrison, P.A., Jäger, J., Rounsevell, M.D.A., Tinch, R., 2015. Exploring climate change vulnerability across sectors and scenarios using indicators of impacts and coping capacity. Clim. Chang. 128:339–354. http://dx.doi.org/10.1007/s10584-014-1162-8.

Duscher, K., Günther, A., Richts, A., Clos, P., Philipp, U., Struckmeier, W., 2015. The GIS layers of the "International Hydrogeological Map of Europe 1:1,500,000" in a vector format. Hydrogeol. J. 23:1867–1875. http://dx.doi.org/10.1007/s10040-015-1296-4.

Fekete, A., 2009. Validation of a social vulnerability index in context to river-floods in Germany. Nat. Hazards Earth Syst. Sci. 9:393–403. http://dx.doi.org/10.5194/nhess-9-393-2009.

Flörke, M., Wimmer, F., Laaser, C., Vidaurre, R., Tröltzsch, J., Dworak, T., Stein, U., Marinova, N., Jaspers, F., Ludwig, F., 2011. Final Report for the Project Climate Adaptation–Modelling Water Scenarios and Sectoral Impacts. CESR-European Comm. Dir. Gen. Environ.

Fraser, E.D.G., Simelton, E., Termansen, M., Gosling, S.N., South, A., 2013. "Vulnerability hotspots": integrating socio-economic and hydrological models to identify where cereal production may decline in the future due to climate change induced drought. Agric. For. Meteorol. 170:195–205. http://dx.doi.org/10.1016/j.agrformet.2012.04.008.

Füssel, H.-M., Klein, R.J.T., 2006. Climate change vulnerability assessments: an evolution of conceptual thinking. Clim. Chang. 75:301–329. http://dx.doi.org/10.1007/s10584-006-0329-3.

Garcia Gonzalez, R., Verhoef, A., Luigi Vidale, P., Braud, I., 2012. Incorporation of water vapor transfer in the JULES land surface model: implications for key soil variables and land surface fluxes. Water Resour. Res. 48. http://dx.doi.org/10.1029/2011WR011811 (n/a–n/a).

González Tánago, I., Urquijo, J., Blauhut, V., Villarroya, F., De Stefano, L., 2016. Learning from experience: a systematic review of assessments of vulnerability to drought. Nat. Hazards 80:951–973. http://dx.doi.org/10.1007/s11069-015-2006-1.

Grillakis, M.G., Koutroulis, A.G., Papadimitriou, L.V., Daliakopoulos, I.N., Tsanis, I.K., 2016. Climate-induced shifts in global soil temperature regimes. Soil Sci. 181, 264–272.

Grillakis, M.G., Koutroulis, A.G., Daliakopoulos, I.N., Tsanis, I.K., 2017. A method to preserve trends in quantile mapping bias correction of climate modeled temperature. Earth Syst. Dyn. Discuss.:1–26 http://dx.doi.org/10.5194/esd-2017-53.

Grouillet, B., Fabre, J., Ruelland, D., Dezetter, A., 2015. Historical reconstruction and 2050 projections of water demand under anthropogenic and climate changes in two contrasted Mediterranean catchments. J. Hydrol. 522:684–696. http://dx.doi.org/10.1016/j.jhydrol.2015.01.029.

Gudmundsson, L., Wagener, T., Tallaksen, L.M., Engeland, K., 2012. Evaluation of nine large-scale hydrological models with respect to the seasonal runoff climatology in Europe. Water Resour. Res. 48. http://dx.doi.org/10.1029/2011WR010911 (n/a–n/a).

Hanasaki, N., Kanae, S., Oki, T., Masuda, K., Motoya, K., Shirakawa, N., Shen, Y., Tanaka, K., 2008. An integrated model for the assessment of global water resources – part 1: model description and input meteorological forcing. Hydrol. Earth Syst. Sci. 12: 1007–1025. http://dx.doi.org/10.5194/hess-12-1007-2008.

Hanasaki, N., Fujimori, S., Yamamoto, T., Yoshikawa, S., Masaki, Y., Hijioka, Y., Kainuma, M., Kanamori, Y., Masui, T., Takahashi, K., Kanae, S., 2013. A global water scarcity assessment under shared socio-economic pathways - part 2: water availability and scarcity. Hydrol. Earth Syst. Sci. 17:2393–2413. http://dx.doi.org/10.5194/hess-17-2393-2013.

Hempel, S., Frieler, K., Warszawski, L., Schewe, J., Piontek, F., 2013. A trend-preserving bias correction – the ISI-MIP approach. Earth Syst. Dynam. 4:219–236. http://dx.doi.org/10.5194/esd-4-219-2013.

Huffman, G.J., Bolvin, D.T., 2013. TRMM and Other Data Precipitation Data Set Documentation.

Huffman, G.J., Adler, R.F., Morrissey, M.M., Bolvin, D.T., Curtis, S., Joyce, R., McGavock, B., Susskind, J., Huffman, G.J., Adler, R.F., Morrissey, M.M., Bolvin, D.T., Curtis, S., Joyce, R., McGavock, B., Susskind, J., 2001. Global precipitation at one-degree daily resolution from multisatellite observations. J. Hydrometeorol. 2:36–50. http://dx.doi.org/10.1175/1525-7541(2001)002<0036:GPAODD>2.0.CO;2.

Huffman, G.J., Bolvin, D.T., Nelkin, E.J., Wolff, D.B., Adler, R.F., Gu, G., Hong, Y., Bowman, K.P., Stocker, E.F., Huffman, G.J., Bolvin, D.T., Nelkin, E.J., Wolff, D.B., Adler, R.F., Gu, G., Hong, Y., Bowman, K.P., Stocker, E.F., 2007. The TRMM multisatellite precipitation analysis (TMPA): quasi-global, multiyear, combined-sensor precipitation estimates at fine scales. J. Hydrometeorol. 8:38–55. http://dx.doi.org/10.1175/JHM560.1.

Iglesias, A., Moneo, M., Quiroga, S., 2009. Methods for evaluating social vulnerability to drought. Coping with Drought Risk in Agriculture and Water Supply Systems. Springer, pp. 153–159.

Kalnay, E., Kanamitsu, M., Kistler, R., Collins, W., Deaven, D., Gandin, L., Iredell, M., Saha, S., White, G., Woollen, J., Zhu, Y., Leetmaa, A., Reynolds, R., Chelliah, M., Ebisuzaki, W., Higgins, W., Janowiak, J., Mo, K.C., Ropelewski, C., Wang, J., Jenne, R., Joseph, D., 1996. The NCEP/NCAR 40-year reanalysis project. Bull. Am. Meteorol. Soc. 77:437–471. http://dx.doi.org/10.1175/1520-0477(1996)077<0437:TNYRP>2.0.CO;2.

Kaufmann, D., Kraay, A., Mastruzzi, M., 2010. The worldwide governance indicators: methodology and analytical issues. The World Bank.

KC, S., Lutz, W., 2014. The human core of the shared socioeconomic pathways: population scenarios by age, sex and level of education for all countries to 2100. Glob. Environ. Chang. http://dx.doi.org/10.1016/j.gloenvcha.2014.06.004.

Kossida, M., Kakava, A., Tekidou, A., Mimikou, M., Iglesias, A., 2012. Vulnerability to water scarcity and drought in Europe: thematic assessment for EEA Water 2012 Report, ETC/ICM Tech. Rep. 3/2012. Eur. Top. Cent. on Inland, Coastal and Mar. Waters.

Koutroulis, A.G., Tsanis, I.K., Daliakopoulos, I.N., Jacob, D., 2013. Impact of climate change on water resources status: a case study for Crete Island, Greece. J. Hydrol. 479:146–158. http://dx.doi.org/10.1016/j.jhydrol.2012.11.055.

Koutroulis, A.G., Grillakis, M.G., Daliakopoulos, I.N., Tsanis, I.K., Jacob, D., 2016. Cross sectoral impacts on water availability at +2°C and +3°C for east Mediterranean island states: the case of Crete. J. Hydrol. 532. http://dx.doi.org/10.1016/j.jhydrol.2015.11.015.

Kovats, R.S., Valentini, R., Bouwer, L.M., Georgopoulou, E., Jacob, D., Martin, E., Rounsevell, M., 2014. J.F. Soussana, 2014: Europe. Climate Change 2014: Impacts, Adaptation, and Vulnerability. Part B: Regional Aspects. Contribution of Working Group II to the Fifth Assessment Report of the Intergovernmental Panel on Climate Change Barros, VR, CB Fie.

Le Vine, N., Butler, A., McIntyre, N., Jackson, C., 2016. Diagnosing hydrological limitations of a land surface model: application of JULES to a deep-groundwater chalk basin. Hydrol. Earth Syst. Sci. 20:143–159. http://dx.doi.org/10.5194/hess-20-143-2016.

Leary, N., Kulkarni, J., 2007. Climate Change Vulnerability and Adaptation in Developing Country Regions Draft Final Report of the AIACC Project. Leary et al. "For Whom the Bell Tolls: Lessons about Climate Change Vulnerability from the AIACC Project".

Lorenzo-Lacruz, J., Vicente-Serrano, S.M., López-Moreno, J.I., Beguería, S., García-Ruiz, J.M., Cuadrat, J.M., 2010. The impact of droughts and water management on various hydrological systems in the headwaters of the Tagus River (central Spain). J. Hydrol. 386: 13–26. http://dx.doi.org/10.1016/j.jhydrol.2010.01.001.

MacKellar, N.C., Dadson, S.J., New, M., Wolski, P., 2013. Evaluation of the JULES land surface model in simulating catchment hydrology in Southern Africa. Hydrol. Earth Syst. Sci. Discuss. 10:11093–11128. http://dx.doi.org/10.5194/hessd-10-11093-2013.

Mckee, T.B., Doesken, N.J., Kleist, J., 1993. The Relationship of Drought Frequency and Duration to Time Scales. pp. 17–22.

Mitchell, K.E., Lohmann, D., Houser, P.R., Wood, E.F., Schaake, J.C., Robock, A., Cosgrove, B.A., Sheffield, J., Duan, Q., Luo, L., Higgins, R.W., Pinker, R.T., Tarpley, J.D., Lettenmaier, D.P., Marshall, C.H., Entin, J.K., Pan, M., Shi, W., Koren, V., Meng, J., Ramsay, B.H., Bailey, A.A., 2004. The multi-institution North American Land Data Assimilation System (NLDAS): utilizing multiple GCIP products and partners in a continental distributed hydrological modeling system. J. Geophys. Res. 109 (D07S90). http://dx.doi.org/10.1029/2003JD003823.

Moss, R.H., Edmonds, J.A., Hibbard, K.A., Manning, M.R., Rose, S.K., van Vuuren, D.P., Carter, T.R., Emori, S., Kainuma, M., Kram, T., Meehl, G.A., Mitchell, J.F.B., Nakicenovic, N., Riahi, K., Smith, S.J., Stouffer, R.J., Thomson, A.M., Weyant, J.P., Wilbanks, T.J., 2010. The next generation of scenarios for climate change research and assessment. Nature 463: 747–756. http://dx.doi.org/10.1038/nature08823.

Mouratiadou, I., Biewald, A., Pehl, M., Bonsch, M., Baumstark, L., Klein, D., Popp, A., Luderer, G., Kriegler, E., 2016. The impact of climate change mitigation on water demand for energy and food: an integrated analysis based on the Shared Socioeconomic Pathways. Environ. Sci. Pol. 64:48–58. http://dx.doi.org/10.1016/j.envsci.2016.06.007.

Naumann, G., Barbosa, P., Garrote, L., Iglesias, A., Vogt, J., 2014. Exploring drought vulnerability in Africa: an indicator based analysis to be used in early warning systems. Hydrol. Earth Syst. Sci. 18:1591–1604. http://dx.doi.org/10.5194/hess-18-1591-2014.

O'Neill, B.C., Kriegler, E., Ebi, K.L., Kemp-Benedict, E., Riahi, K., Rothman, D.S., van Ruijven, B.J., van Vuuren, D.P., Birkmann, J., Kok, K., Levy, M., Solecki, W., 2015. The roads ahead: narratives for shared socioeconomic pathways describing world futures in the 21st century. Glob. Environ. Chang. http://dx.doi.org/10.1016/j.gloenvcha.2015.01.004.

Pacifico, F., Harrison, S.P., Jones, C.D., Arneth, A., Sitch, S., Weedon, G.P., Barkley, M.P., Palmer, P.I., Serça, D., Potosnak, M., Fu, T.-M., Goldstein, A., Bai, J., Schurgers, G., 2011. Evaluation of a photosynthesis-based biogenic isoprene emission scheme in JULES and simulation of isoprene emissions under present-day climate conditions. Atmos. Chem. Phys. 11:4371–4389. http://dx.doi.org/10.5194/acp-11-4371-2011.

Panagos, P., Ballabio, C., Meusburger, K., Spinoni, J., Alewell, C., Borrelli, P., 2017. Towards estimates of future rainfall erosivity in Europe based on REDES and WorldClim datasets. J. Hydrol. 548:251–262. http://dx.doi.org/10.1016/j.jhydrol.2017.03.006.

Papadimitriou, L.V., Koutroulis, A.G., Grillakis, M.G., Tsanis, I.K., 2015. High-end climate change impact on European water availability and stress: exploring the presence of biases. Hydrol. Earth Syst. Sci. Discuss. 12:7267–7325. http://dx.doi.org/10.5194/hessd-12-7267-2015.

Papadimitriou, L.V., Koutroulis, A.G., Grillakis, M.G., Tsanis, I.K., 2016. High-end climate change impact on European runoff and low flows: exploring the effects of forcing biases. Hydrol. Earth Syst. Sci. 20:1785–1808. http://dx.doi.org/10.5194/hess-20-1785-2016.

Parry, M.L., 2007. Climate Change 2007: Impacts, Adaptation and Vulnerability: Contribution of Working Group II to the Fourth Assessment Report of the Intergovernmental Panel on Climate Change. Cambridge University Press.

Penman, H.L., 1948. Natural evaporation from open water, bare soil and grass. Proceedings of the Royal Society of London A: Mathematical, Physical and Engineering Sciences, pp. 120–145.

Perčec Tadić, M., Gajić-Čapka, M., Zaninović, K., Cindrić, K., 2014. Drought vulnerability in Croatia. Agric. Conspec. Sci. 79, 31–38.

Preston, B.L., Scientific, C., 2008. Mapping Climate Change Vulnerability in the Sydney Coastal Councils Group (CSIRO and Sydney Coastal Councils Group).

Prudhomme, C., Parry, S., Hannaford, J., Clark, D.B., Hagemann, S., Voss, F., 2011. How well do large-scale models reproduce regional hydrological extremes in Europe? J. Hydrometeorol. 12:1181–1204. http://dx.doi.org/10.1175/2011JHM1387.1.

Richards, L.A., 1931. Capillary conduction of liquids through porous mediums. J. Appl. Phys. 1, 318–333.

Roudier, P., Andersson, J.C.M., Donnelly, C., Feyen, L., Greuell, W., Ludwig, F., 2016. Projections of future floods and hydrological droughts in Europe under a +2°C global warming. Clim. Chang. 135:341–355. http://dx.doi.org/10.1007/s10584-015-1570-4.

Russo, A., Smith, I., Atkinson, R., Servillo, L.A., Madsen, B., Van den Borg, J., 2012. ATTREG. The Attractiveness of European Regions and Cities for Residents and Visitors-Scientific Report. Status Publ.

Salvati, L., Zitti, M., Ceccarelli, T., Perini, L., 2009. Developing a synthetic index of land vulnerability to drought and desertification. Geogr. Res. 47, 280–291.

Sheffield, J., Goteti, G., Wood, E.F., 2006. Development of a 50-year high-resolution global dataset of meteorological forcings for land surface modeling. J. Clim. 19:3088–3111. http://dx.doi.org/10.1175/JCLI3790.1.

SHEN, Y., OKI, T., UTSUMI, N., KANAE, S., HANASAKI, N., 2010. Projection of Future World Water Resources Under SRES Scenarios: Water Withdrawal (Projection des ressources en eau mondiales futures selon les scénarios du RSSE: prélèvement d'eau). http://dx.doi.org/10.1623/hysj.53.1.11.

Shukla, S., Wood, A.W., 2008. Use of a standardized runoff index for characterizing hydrologic drought. Geophys. Res. Lett. 35, L02405. http://dx.doi.org/10.1029/2007GL032487.

Slevin, D., Tett, S.F.B., Williams, M., 2014. Multi-site evaluation of the JULES land surface model using global and local data. Geosci. Model Dev. Discuss. 7:5341–5380. http://dx.doi.org/10.5194/gmdd-7-5341-2014.

Smit, B., Wandel, J., 2006. Adaptation, adaptive capacity and vulnerability. Glob. Environ. Chang. 16:282–292. http://dx.doi.org/10.1016/j.gloenvcha.2006.03.008.

Stackhouse Jr., P.W., SK, G., SJ, C., Chiacchio, M., Mikovitz, J., 2000. The WCRP/GEWEX Surface Radiation Budget Project Release 2: An Assessment of Surface Fluxes at 1 Degree Resolution.

Stagge, K.S., 2015. Methodological Approach Considering Different Factors Influencing Vulnerability–Pan-European Scale.

Stagge, J.H., Tallaksen, L.M., Gudmundsson, L., Van Loon, A.F., Stahl, K., 2015. Candidate distributions for climatological drought indices (SPI and SPEI). Int. J. Climatol. 35: 4027–4040. http://dx.doi.org/10.1002/joc.4267.

Stigter, T.Y., Varanda, M., Bento, S., Nunes, J.P., Hugman, R., 2017. Combined assessment of climate change and socio-economic development as drivers of freshwater availability in the south of Portugal. Water Resour. Manag. 31:609–628. http://dx.doi.org/10.1007/s11269-015-0994-y.

Turner, B.L., Kasperson, R.E., Matson, P.A., McCarthy, J.J., Corell, R.W., Christensen, L., Eckley, N., Kasperson, J.X., Luers, A., Martello, M.L., Polsky, C., Pulsipher, A., Schiller, A., 2003. A framework for vulnerability analysis in sustainability science. Proc. Natl. Acad. Sci. U. S. A. 100:8074–8079. http://dx.doi.org/10.1073/pnas.1231335100.

Vautard, R., Gobiet, A., Sobolowski, S., Kjellström, E., Stegehuis, A., Watkiss, P., Mendlik, T., Landgren, O., Nikulin, G., Teichmann, C., Jacob, D., 2014. The European climate under a 2 °C global warming. Environ. Res. Lett. 9:34006. http://dx.doi.org/10.1088/1748-9326/9/3/034006.

Veldkamp, T.I.E., Wada, Y., Aerts, J.C.J.H., Ward, P.J., 2016. Towards a global water scarcity risk assessment framework: incorporation of probability distributions and hydro-climatic variability. Environ. Res. Lett. 11:24006. http://dx.doi.org/10.1088/1748-9326/11/2/024006.

Wada, Y., Flörke, M., Hanasaki, N., Eisner, S., Fischer, G., Tramberend, S., Satoh, Y., van Vliet, M.T.H., Yillia, P., Ringler, C., Burek, P., Wiberg, D., 2016. Modeling global water use for the 21st century: the Water Futures and Solutions (WFaS) initiative and its approaches. Geosci. Model Dev. 9:175–222. http://dx.doi.org/10.5194/gmd-9-175-2016.

Yohe, G., Tol, R.S.J., 2002. Indicators for social and economic coping capacity—moving toward a working definition of adaptive capacity. Glob. Environ. Chang. 12:25–40. http://dx.doi.org/10.1016/S0959-3780(01)00026-7.

Zulkafli, Z., Buytaert, W., Onof, C., Lavado, W., Guyot, J.L., 2013. A critical assessment of the JULES land surface model hydrology for humid tropical environments. Hydrol. Earth Syst. Sci. 17:1113–1132. http://dx.doi.org/10.5194/hess-17-1113-2013.